

# Phototransduction in Rods and Cones

Yingbin Fu, PhD<sup>1</sup>

Created: April 1, 2010.

## 1. Introduction

Vertebrates rely on retinal rods and cones for the conventional, image-forming vision while non-image-forming vision is mediated by intrinsically photosensitive retinal ganglion cells (ipRGCs) (see [chapter on Melanopsin Ganglion Cells](#)). Rods are specialized for low-light vision. They are extremely sensitive and can signal the absorption of single photons. Cones mediate daylight vision (Figure 1). They are much less sensitive to light than rods, but have higher temporal resolution. They also mediate color vision by several cone types with different pigment spectra sensitivity.

Great progress has been made in understanding rod phototransduction since the introduction of the suction-electrode recording technique in the late 1970s (1). Individual amphibian and mammalian (including primate) photoreceptors can be recorded with this method. Bovine retina, on the other hand, has been a favorite preparation for studying phototransduction by biochemists because of the abundance of tissue available. The mouse, however, has become an increasingly popular animal model for study in the past decade through the advent of gene-targeting techniques. When combined with electrophysiology, mouse genetics provides unmatched power in elucidating the *in vivo* functions of key phototransduction proteins, most of which have been knocked out, overexpressed or mutated in rods, yielding a rich body of information on the mechanisms underlying the amplification, recovery and adaptation of rod/cone photoresponses (Table 1, Figure 2, Figure 3).

I shall first give a brief description of the structure and the development of mouse photoreceptors, followed by a summary of recent studies on rod phototransduction with emphasis on information gleaned from mouse models. Finally, a recent advance in studying mouse cones will be mentioned.

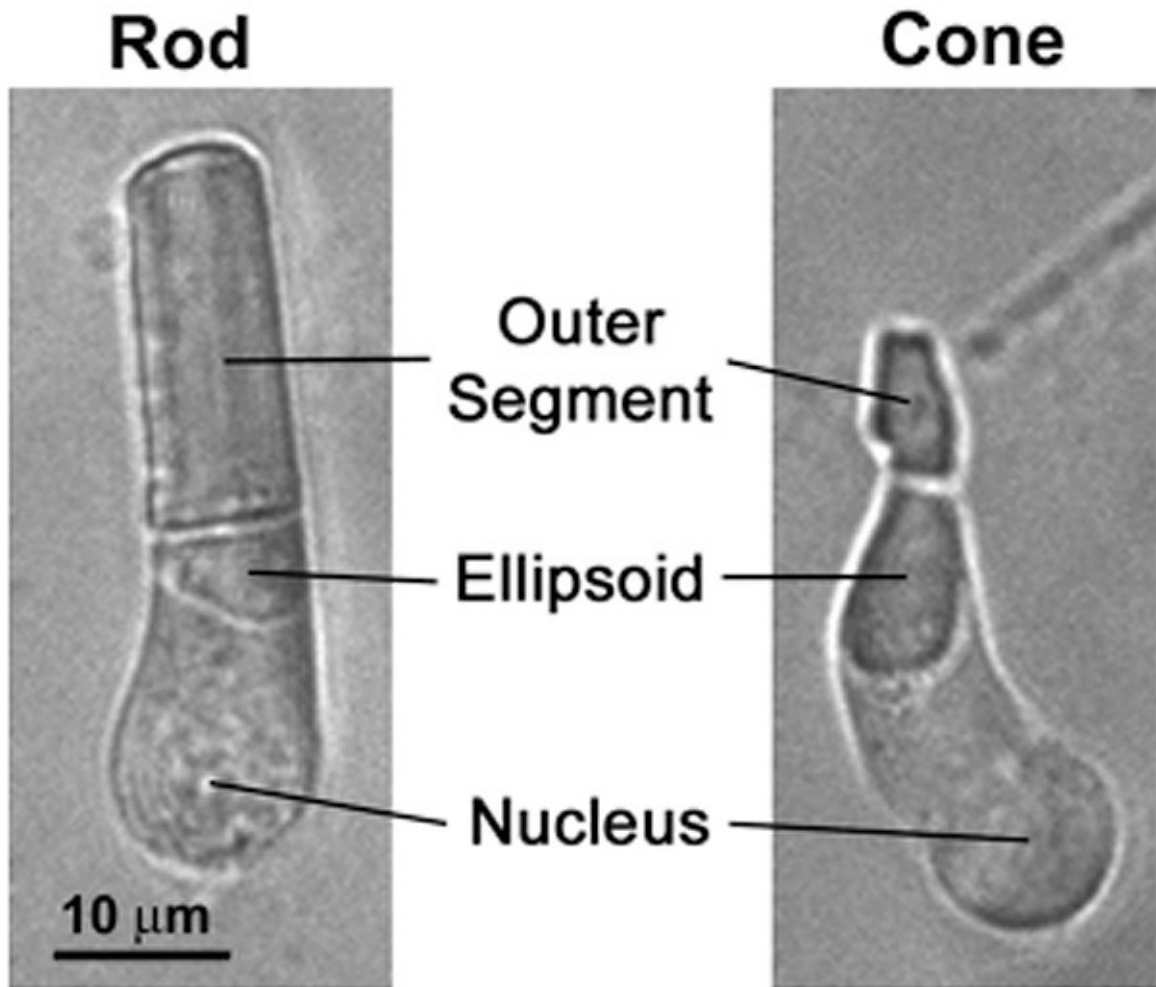


Figure 1. Brightfield images of living rod and cone photoreceptors isolated from a salamander retina. Phototransduction takes place in the outer segment, while the ellipsoid is densely packed with mitochondria. Rods are responsible for dim light vision, cones for bright light vision. Courtesy of Yiannis Koutalos.

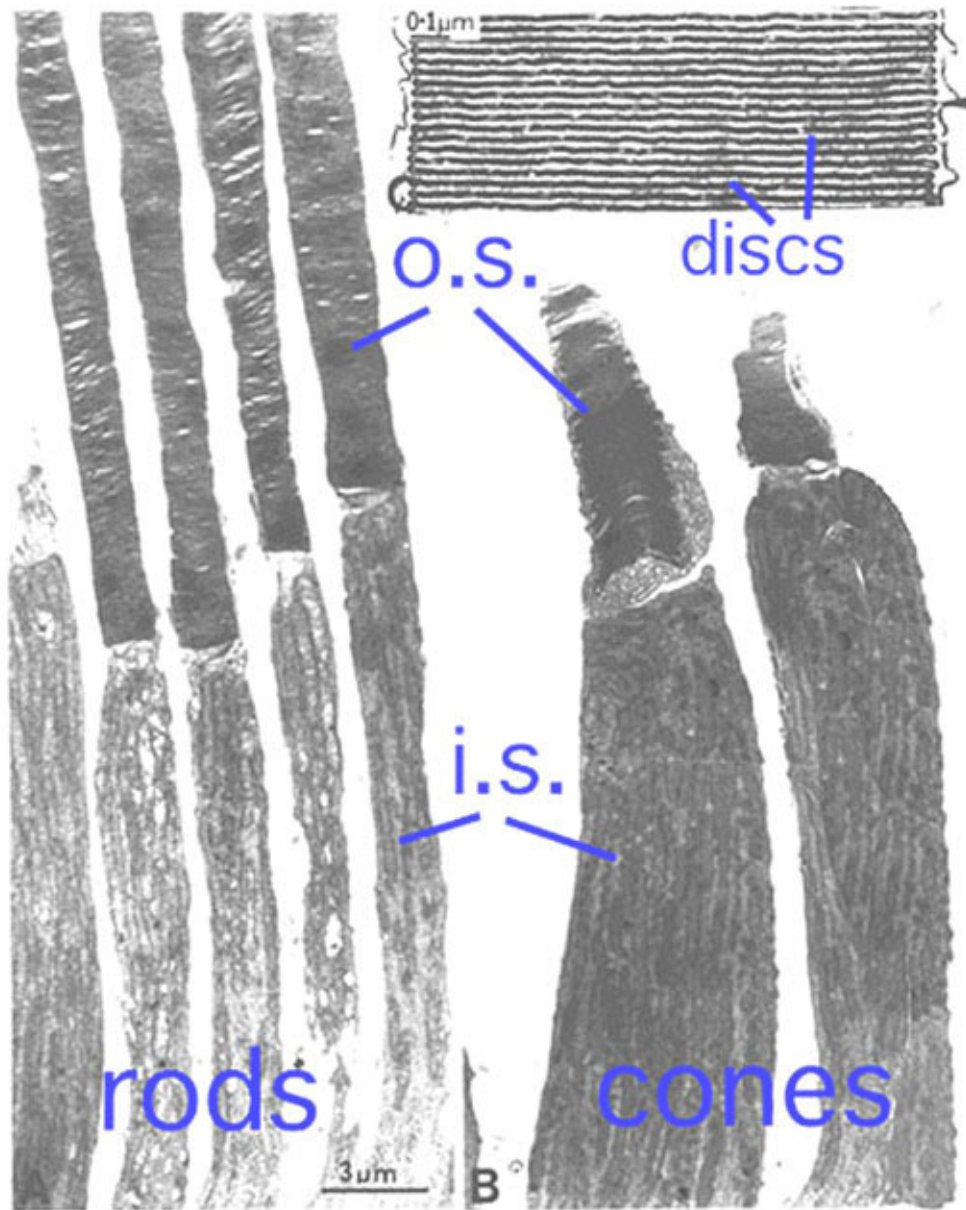


Figure 2. Low magnification EM image of monkey rods and cones with an enlargement of the outer segment discs.

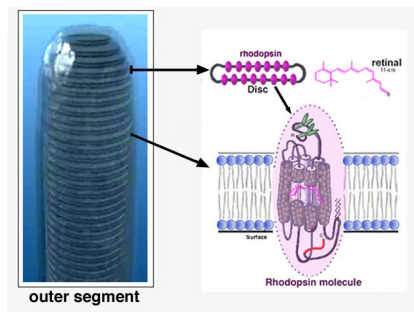


Figure 3. Schematic diagram of rhodopsin in the outer segment discs. When the outer segments are magnified further, stacked membrane disks are visible inside. The disks are studded with thousands of rhodopsin complexes. Each rhodopsin consists of a membrane-traversing protein with a retinal molecule embedded in its core.

Table 1. List of major proteins involved in mouse rod and cone phototransductions that have been knocked out, overexpressed or mutated.

Proteins	Manipulation	Phenotype	References
Rhodopsin	knockout	no ROS formation, no rod photoresponse	Humphries et al., 1997; Lem et al., 1999 (3, 4)
Transducin G $\alpha_{t1}$	knockout	no rod photoresponse	Calvert et al., 2000 (85)
Transducin G $\alpha_{\gamma 1}$	knockout	down regulation of G $\alpha_{t1}$ & G $\beta_1$ , reduced rod sensitivity, retinal degeneration	Lobanova et al., 2008 (210)
Transducin G $\alpha_{\gamma 1}$	S70L mutation	deficit in light adaptation in rods	Kassai et al., 2005 (90)
phosducin	knockout	reduced rod sensitivity	Krispel et al., 2007 (211)
PDE $\beta$	mutation	rd mouse, retinal degeneration	Bowes et al., 1990; Pittler and Baehr, 1991(105, 106)
PDE $\gamma$	knockout	reduced PDE activity, retinal degeneration	Tsang et al., 1996 (102)
PDE $\gamma$	overexpression	reduced gain, accelerated shutoff in rods	Tsang et al., 2006 (212)
PDE $\gamma$	W70A	reduced sensitivity, slow shutoff in rods	Tsang et al., 1998 (109)
CNGB1	knockout	no rod photoresponse, retinal degeneration	Huttl et al., 2005; Zhang et al., 2009 (127, 213)
CNGA3	knockout	no cone photoresponse, slow cone degeneration	Biel et al., 1999a (121)
GRK1	knockout	slow shutoff in rods & cones	Chen et al., 1999; Nikonov et al., 2005 (139, 146)
GRK1	overexpression	normal rod photoresponse	Krispel et al., 2006 (77)
Arrestin1	knockout	slow shutoff in rods	Xu et al., 1997 (155)
Arrestin1& 42	Double knockout	slow shutoff in rods and cones	Nikonov et al., 2008 (168)
Recoverin	knockout	reduced rod sensitivity, decreased signal transfer between rods and rod bipolar cells	Makino et al., 2004; Sampath et al., 2005 (154, 214)
RGS9-13	overexpression	accelerated shutoff in rods	Krispel et al., 2006 (77)
RGS9-1	knockout	slow shutoff in rods and cones	Chen et al., 2000; Lyubarsky et al., 2001 (172, 215)
G $\beta_5$ -L	knockout	same as RGS9-1 knockout	Krispel et al., 2003b (180)
R9AP	knockout	same as RGS9-1 knockout	Keresztes et al., 2004 (174)
GC1	knockout	normal rod response, no cone response, cone dystrophy	Baehr et al., 2007; Yang et al., 1999 (187, 188)
GC2	knockout	Normal rod & cone responses	Baehr et al., 2007 (187)
GC1 & 2	Double knockout	No light response in rods & cones, cone degeneration	Baehr et al., 2007 (187)
GCAP2	knockout	Rods recover more slowly, more sensitive to flashes, saturate at lower intensities	Makino et al., 2008 (200)

Table 1. continued from previous page.

GCAP1 & 2	Double knockout	larger amplitude, delayed recovery in rods and cones	Mendez et al., 2001; Pennesi et al., 2003 (193, 199)
-----------	-----------------	--	--

1 Due to space limitation, not all the genetically engineered mouse lines are listed. For those included, only the most salient phenotypes are listed, please refer to the text for more complete description.

2 Arrestin4 is also called cone arrestin or X-arrestin (168, 216).

3 RGS9-1 overexpression was achieved by overexpressing R9AP, which resulted in overexpression of all three components of the GAP complex, RGS9-1, Gβ5-L and R9AP.

## 2. Structure of rods and cones.

Rods constitute ~97% of mouse retinal photoreceptors, with cones accounting for the remainder (2). The mouse photoreceptors are broadly similar to primate photoreceptors in physical dimensions (Table 2, Figure 2). The outer segment is about 1.4 μm in diameter and 24 μm in length for rods, and, correspondingly, about 1.2 μm and 13 μm for cones. These dimensions are significantly smaller than those of amphibian photoreceptors (Figure 1), which explain physiologists' longtime favor for the latter.

Rods and cones have four primary structural/functional regions: outer segment, inner segment, cell body and synaptic terminal. The outer segment is connected to the inner segment through a thin connecting cilium. The outer segment is filled with a dense stack of membrane discs (Figure 2 and Figure 3), spaced at intervals of about 28 nm. The discs carry the visual pigment (rhodopsin in rods and cone pigment in cones) and other transduction components either as transmembrane or peripheral membrane proteins (Figure 3). Visual pigment is the most abundant protein in the outer segment. The importance of visual pigment as a major structural component is demonstrated by the rhodopsin-knockout mouse, the rod outer segments of which fail to form (3, 4). The rod photoreceptors of this mouse degenerate, followed suit by cones. The packing density of pigment molecules on the discs is remarkably uniform across different vertebrate species, being ~25000 mm<sup>2</sup>, corresponding to a concentration of ~ 3mM (5). The total number of pigment molecules in the outer segment can thus be calculated roughly from its envelope volume. The dense stack of discs greatly increases the probability of photon capture. An interesting difference between rods and cones is that the rod discs (except for the nascent discs at the base of the outer segment) are completely internalized and therefore physically separate from the plasma membrane, whereas the cone discs remain as foldings of the plasma membrane. The open cone discs offer a much larger surface area for rapid fluxes of substances between the cell exterior and interior, such as chromophore transfer for pigment regeneration and fast calcium dynamics during light adaptation.

The inner segment contains the endoplasmic reticulum and the Golgi apparatus. It is also packed with mitochondria immediately adjacent to the outer segment (Figure 2, Figure 3) in order to meet the high demand for metabolic energy associated with phototransduction. All proteins destined for the outer segment must pass through a narrow connecting cilium between the outer and the inner segments.

The synaptic terminal transmits the light signal to the second-order neurons in the retina: the bipolar and horizontal cells. In darkness, there is a steady inward current (the "dark current") through a cation conductance on the outer-segment membrane (6), depolarizing the rod or cone and maintaining a steady synaptic release of glutamate. Light closes this cation conductance (the "light-sensitive" conductance, consisting of cGMP-gated channels) to stop the dark current and produce a membrane hyperpolarization as the response. This hyperpolarization decreases or terminates the dark glutamate release. The signal is further processed by other neurons in the retina before being transmitted to higher centers in the brain.

Table 2. Physical dimensions of the outer segment of mouse rods and cones. Salamander and primate photoreceptors are included for comparison purpose.

		Rods			Cones	
--	--	------	--	--	-------	--

Table 2. continued from previous page.

	Mouse	Primate	Salamander	Mouse	Primate	Salamander
Length ( $\mu\text{m}$ )	23.6	25	22	13.4	13	8
Diameter <sup>a</sup> ( $\mu\text{m}$ )	1.4	2	11	1.2	3 <sub>base</sub> , 1 <sub>tip</sub>	4 <sub>base</sub> , 2.5 <sub>tip</sub>
Volume ( $\mu\text{m}^3$ )	36	40	2000	14	30	70
References	Carter-Dawson and LaVail, 1979 (2)	Baylor et al., 1984 (217)	Baylor and Nunn, 1986 (218)	Carter-Dawson and LaVail, 1979 (2)	Pugh and Lamb, 2000 (101)	Pugh and Lamb, 2000 (101)

### 3. Can we see a single photon?

The minimum number of photons required to produce a visual effect was first successfully determined by Hecht, Schlaer and Pirenne in a landmark experiment (7). Human subjects were allowed to stay in the dark for 30 minutes to have optimal visual sensitivity. The stimulus was presented 20 degrees to the left of the point of focus so that the light would fall on the region of the retina with the highest concentration of rods. The stimulus was a circle of red light with a diameter of 10 minutes (1 minute=1/60th of a degree). The subjects were asked whether they had seen a flash. The light was gradually reduced in intensity until the subjects could only guess the answer. It was found that between 54 and 148 photons were required in order to elicit visual experience. After corrections for corneal reflection (4%), ocular media absorption (50%) and photons passed through retina (80%), only 5 to 14 photons were actually absorbed by the retinal rods. The small number of photons in comparison with the large number of rods (500) involved makes it very unlikely that any rod will take up more than one photon. Therefore, one photon must be absorbed by each of 5 to 14 rods in the retina to produce a visual effect.

In the same publication (7), Hecht and co-workers determined the visual threshold of human vision by the famous "frequency-of-seeing-curves" experiment. The theory is that photon absorptions vary according to a Poisson probability distribution. If  $a$  is the average number of photons absorbed per flash, the probability  $P_n$  that any number  $n$  will be absorbed is:  $P_n = a^n / (e^a n!)$ . Some of these Poisson integral curves ( $n$  from 1 to 9) are shown in Figure 4. By measuring the frequency of seeing against the logarithm of the brightness experimentally, one can fit the experimental curve with one of the probability distribution in Figure 4b to reveal the value  $n$ , which lies between 5 and 8 (Figure 4b). This agrees well with the value 5 to 14 photons absorbed by rods!

### 4. Development of mouse photoreceptors

Rods and cones renew their outer segments continually (8, 9). Newly formed disks at the base of the outer segment progressively displace previously synthesized disks toward the apical end. The disks reaching the apex of the outer segment are shed and phagocytosed on a daily basis by the adjacent retinal pigment epithelium (RPE) (10). The rate of formation and disposal of the disks are roughly equal so that a constant outer-segment length is maintained in the adult retina.

The mouse rod outer segment (ROS) changes little in diameter during development, but it elongates at a rapid and almost linear rate from postnatal day (P) 11 to 17, reaching adult length by P19-25 (11). The increase in ROS length parallels the almost linear rise in rhodopsin content from P8 to P23 (12). At the peak rate of growth during P13-P17, ~120 disks are synthesized per day compared with 75 disks in adult retina (8, 11).

The dark current recorded in developing mouse rods increases roughly in direct proportion to the length of the mouse ROS between P12 (around the time of eye-opening in neonate) and P45 (adult) (13). The kinetics of the dim-flash response changes rather little during development and the flash sensitivity of rods increases by approximately 1.5-fold, reflecting the presence in neonatal rods of a small percentage (~1%) of free opsin (i.e.

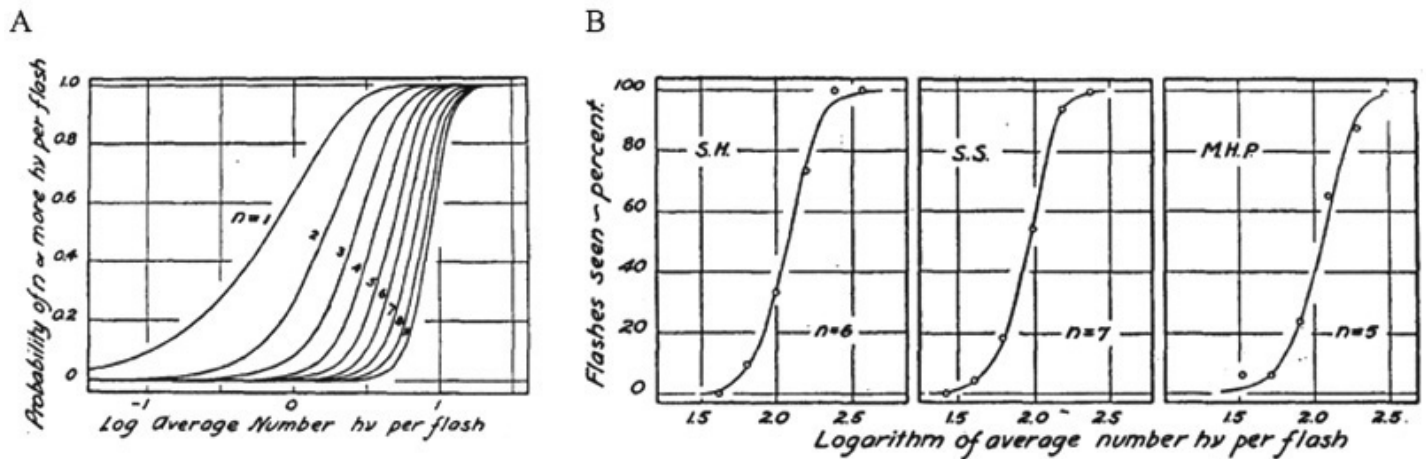


Figure 4. Frequency of seeing curve experiment. (A) Poisson probability distribution. For any average number of quanta ( $h\nu$ ) per flash, the ordinates give the probabilities that the flash will deliver to the retina  $n$  or more photons, depending on the value assumed for  $n$ . (B) Relation between the average energy content of a flash of light (in number of ( $h\nu$ )) and the frequency with which it is seen by three observers. From Figs. 6 & 7 of Hecht et al (7).

devoid of chromophore) even after overnight dark-adaptation. The constitutive activity of this small amount of opsin mildly triggers adaptation mechanisms and therefore causes a small reduction in the sensitivity of the cell (see later). A similar small, age-dependent increase in rod sensitivity was found for rat. Previously, a 50-fold increase in rod sensitivity was reported for rat from neonate to adulthood (14), but now this appears to be incorrect.

## 5. Vertebrate rods are highly efficient photon detectors

Psychophysical experiments performed by Hecht, Schlaer and Pirenne in 1942 suggested that human retinal rods can detect single photons (7) (Figure 4). Thirty seven years later, suction pipette recordings from isolated toad rods by Baylor, Lamb and Yau confirmed this remarkable ability of vertebrate rods (Figure 5) (15). The amazing ability of vertebrate rods to detect single photons can be attributed to at least three factors: high quantum efficiency of photoactivation, low intrinsic noise, and a powerful signal amplification cascade. Two other factors greatly increase the photon capture ability of vertebrate rods, numerical dominance of rods over cones and a highly specialized outer segment structure. The dense stack of discs of the rod outer segment ensures that virtually every photon traveling axially will be captured. In a sense, vertebrate rods can be viewed as sophisticated three-dimensional photon capture devices.

## 6. Phototransduction in rods: a G-protein-signaling pathway

Rod phototransduction is one of the best-characterized G-protein-signaling pathways (Figure 6, Figure 7, Figure 8). The receptor is rhodopsin (R), the G protein is transducin (G), and the effector is cGMP phosphodiesterase (PDE or PDE6). Upon photon absorption, the rhodopsin molecule becomes enzymatically active ( $R^*$ ) and catalyzes the activation of the G protein transducin to  $G^*$ . Transducin, in turn, activates the effector phosphodiesterase (PDE) to  $PDE^*$ .  $PDE^*$  hydrolyzes the diffusible messenger cGMP. The resulting decrease in the cytoplasmic free cGMP concentration leads to the closure of the cGMP-gated channels on the plasma membrane. Channel closure leads to localized reduction on the influx of cations into the outer segment, which results in membrane hyperpolarization, i.e. the intracellular voltage becoming more negative (Figures 6).) This hyperpolarization decreases or terminates the dark glutamate release at the synaptic terminal. The signal is further processed by other neurons in the retina before being transmitted to higher centers in the brain.

This phototransduction cascade is shown in Figures 6 and 7.

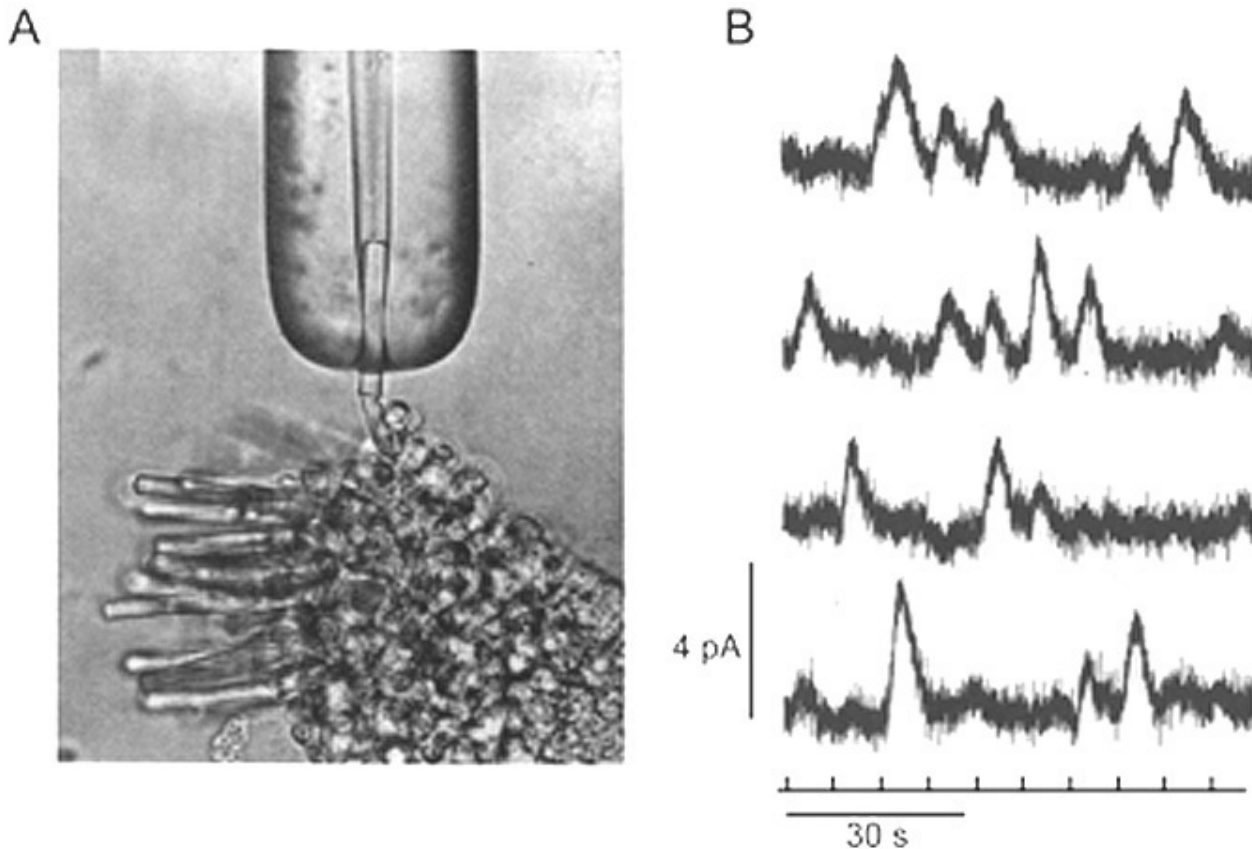


Figure 5. Suction-electrode recording on the membrane current of a single toad rod. (A) The outer segment of a rod projecting from a piece of retina was sucked in position in a suction electrode. Proximal end of cell remains attached to retina. Boundary between inner and outer segments is visible. (B) Response of rod outer segment to a series of 40 consecutive dim flashes. 20 msec flash delivering  $0.029 \text{ photons } \mu\text{m}^{-2}$  at 500 nm, flash timing monitored below. The rod showed no response to some flashes, or a small response of  $\sim 1 \text{ pA}$  to others, and occasionally a larger response. This suggests that the flash response is quantized, as might be expected when on average very few photons are absorbed. With further analysis, the authors demonstrated that each quantal electrical event resulted from a single photo-isomerization with mean amplitude of  $\sim 1 \text{ pA}$  - the single-photon response. Modified from Baylor et al. (15)

Following light activation, a timely recovery of the photoreceptor is essential so that it can respond to subsequently absorbed photons, and signal rapid changes in illumination (Figure 8). This recovery from light requires the efficient inactivation of each of the activated components:  $R^*$ ,  $G^*$ , and  $PDE^*$ , as well as the efficient regeneration of rhodopsin (R) and the rapid restoration of the cGMP concentration. The termination rates of the activation steps set the time course of the photoresponse.

Although rod phototransduction is the best characterized sensory transduction pathway, rods differ from other sensory cells in that light leads to hyperpolarization rather than depolarization. Rods respond to light with graded hyperpolarization whose amplitude increases monotonically as a function of flash intensity until saturation. One hallmark of rod phototransduction is the reproducibility of its single-photon response in both amplitude and kinetics. This is quite remarkable considering the fact that events generated by single molecules are stochastic in nature. The study on the underlying mechanisms has long been a hot topic in the vision field. Recent research pointed to two possible mechanisms: 1. Rhodopsin inactivation is averaged over multiple shutoff steps so that the integrated  $R^*$  activity varies less than otherwise controlled by a single step. 2. Averaging over the deactivation of multiple G protein molecules is important for the constancy in response decay.

The details of the activation phase of rod phototransduction are now well established. A quantitative description is achieved that reproduces the activation kinetics of the rod response under physiological conditions (16-19).



We shall discuss below the major proteins mediating the activation phase in mouse rods - visual pigment, transducin, the effector PDE, and the cGMP-gated channel. The focus will be on studies with combined approaches from mouse genetics and physiology.

## 7. Visual Pigments of Mouse Rods and Cones

Mouse has a single rod pigment, rhodopsin, and two cone pigments: S- and M- cone pigments, with maximal spectral sensitivity at 360 nm and 508 nm, respectively. Mouse is unusual in that individual cones express both S- and M-cone pigments, with the M-pigment level decreasing in a gradient from dorsal to ventral retina (20).

Mouse rhodopsin and cone pigments belong to the super family of G-protein coupled receptors (GPCRs). A high-resolution (2.8 Å), three-dimensional structure of the ground state of bovine rhodopsin was determined in 2000 by Palczewski et al. (Figure 9a) (21, 22). The future challenge is to solve the structure of cone pigments, which is much more unstable than rhodopsin.

Visual pigments from most vertebrate species, including mammals, use 11-cis-retinal (denoted A1), while those from many water-based animals use 11-cis-3,4-dehydroretinal (denoted A2), as their natural ligand (23-25). George Wald first identified vitamin A in the retina (26) and later showed how it functions with light, which forms the molecular basis of vision (Nobel Prize 1967). The chromophore is covalently bound via a Schiff-base linkage to a conserved lysine residue (K296 in mammalian rhodopsin) in the seventh transmembrane helix (Figure 9a and 9b). In darkness, the 11-cis-retinal acts as an inverse agonist to lock rhodopsin in an inactive state by preventing free opsin from activating the transduction cascade. The "locking" role of 11-cis-retinal as was clearly demonstrated in RPE65-null mice. RPE65 functions as an isomerase in the RPE visual cycle, which is important for regenerating rod and cone pigments. Rpe65<sup>-/-</sup> retina has virtually no 11-cis-retinal (27). Rod photoreceptors degenerate slowly due to the constant activation of phototransduction by the large amount of free rod opsin. This degeneration can be prevented by deleting the transducin  $\alpha$ -subunit, which blocks the activation of the downstream cascade (28). In a separate experiment, K296 is mutated to glutamic acid, producing an opsin with no chromophore-binding site (29). Although the K296E opsin constitutively activates transducin in vitro, the constitutive activity of the mutant opsin in vivo was turned off due to phosphorylation by rhodopsin kinase followed by arrestin binding (see R\* termination).

Even with 11-cis-retinal attached, rhodopsin occasionally undergoes spontaneous (thermal) activation in the dark, producing responses identical to those triggered by photons (30). Spontaneous activation of visual pigment molecules sets an ultimate limit on visual sensitivity (31-34). In a toad rod, the rate of thermal activation of rhodopsin was measured to be  $0.031 \text{ s}^{-1} \text{ rod}^{-1}$  at 22 °C, corresponding to an average wait of 2000 years for the spontaneous activation of a given rhodopsin molecule to occur, based on a total of  $2 \times 10^9$  rhodopsin molecules per cell (35). This great stability makes it possible for rods to pack many rhodopsin molecules to the rod discs to increase their photon-capture ability while keeping the dark noise low. In wild-type mouse rods, it is rather difficult to measure the discrete noise arising from the thermal activation of rhodopsin because of the relatively small amplitude of the single-photon response. However, the measurement has been achieved with GCAPs<sup>-/-</sup> rods (36), the single-photon response of which is nearly five times that of wild type as a result of the elimination of the Ca<sup>2+</sup>-mediated negative feedback on guanylate cyclase (see later). The rate is  $\sim 0.012 \text{ s}^{-1} \text{ rod}^{-1}$  at 36°C.

It should be mentioned that the question of dark noise in vision has had a long intellectual history from the point of view of psychophysics and system neuroscience. As early as 1940s and 1950s, Hecht and Barlow have estimated the amount of "dark light" in human rods based on psychophysical experiments (7, 37). More than 30 years later, Baylor and colleagues used suction-pipette recording technique on primate rods to demonstrate that the very low quantal noise from rhodopsin, corresponding to  $\sim 0.01 \text{ event s}^{-1} \text{ rod}^{-1}$  in darkness, indeed matches the human psychophysical scotopic threshold. The quantitative agreement between the quantal noise measured from single rods and that measured in human psychophysics was considered a breakthrough in the

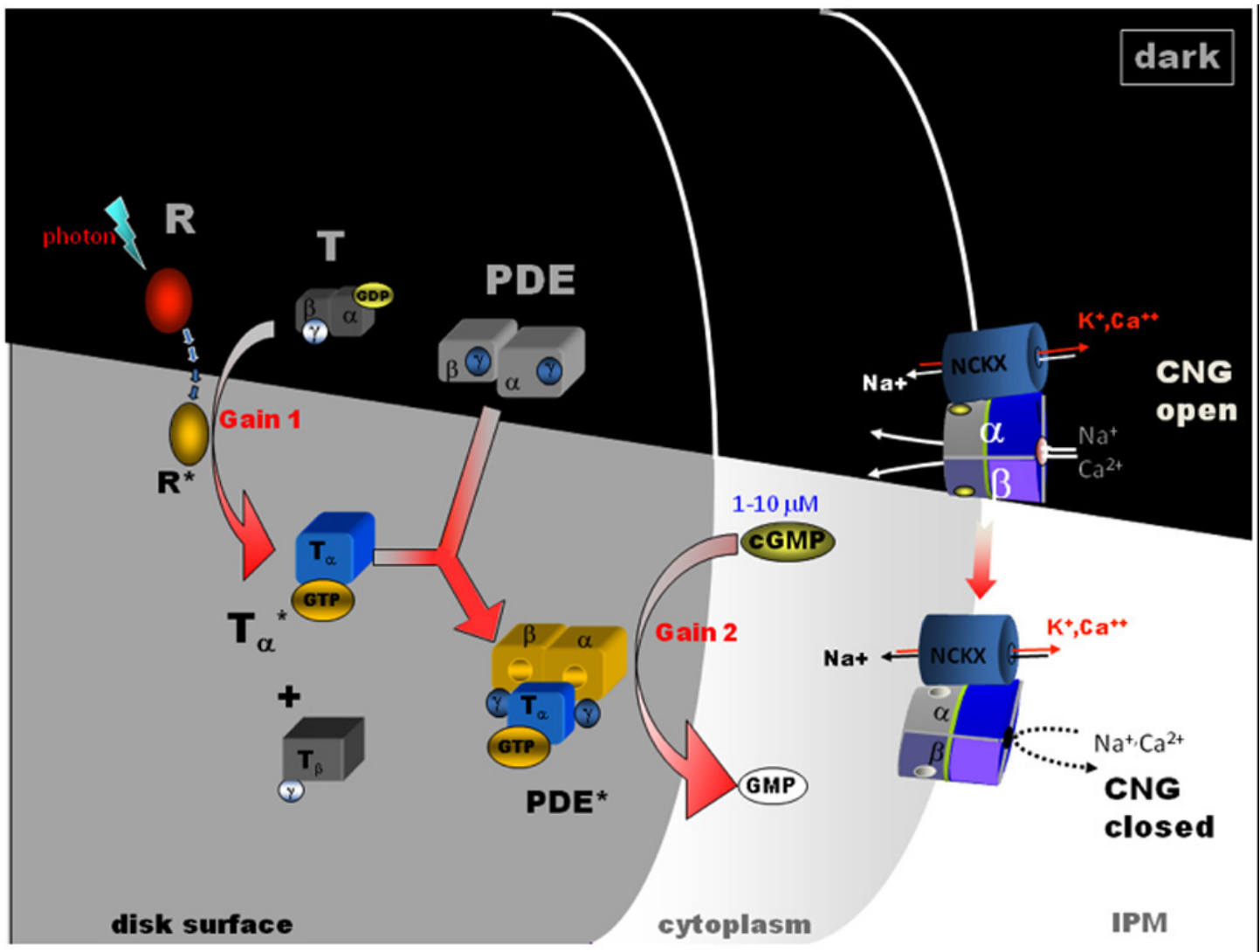


Figure 6. Activation of rod phototransduction cascade that results in the closure of cGMP-gated channels on the plasma membrane (from dark to light state). R, rhodopsin (inactive); R\*, rhodopsin (active); T, transducin; PDE, phosphodiesterase (inactive); PDE\*, phosphodiesterase (active); NCKX, Na/Ca,K exchanger. IPM, interphotoreceptor matrix. Courtesy of Wolfgang Baehr.

vision field and a wonderful convergence between cell physiology and human psychophysics/systems neuroscience - the goal of modern neuroscience after all!

Red cone pigment is much more prone to spontaneous isomerization than rhodopsin (38, 39), but it is difficult to measure the rate from native cones (38). By expressing human red cone pigment transgenically in GCAPs<sup>-/-</sup> rods, the rate of human red cone pigment was found to be surprisingly low at  $\sim 10 \text{ s}^{-1} \text{ cone}^{-1}$  (molecular rate constant  $\sim 1.35 \times 10^{-7} \text{ sec}^{-1}$ ) (40), almost 1000-fold lower than the overall dark transduction noise previously reported in primate cones (41, 42). Thus, the overwhelming amount of dark noise in the primate red cone originates not from spontaneous isomerization of the pigment, but most probably from constitutive activity in the downstream phototransduction steps, such as the phosphodiesterase (43).

The molecular rate constant for thermal isomerization of A2 human red cone pigment was determined to be  $\sim 5.6 \times 10^{-6} \text{ sec}^{-1}$  by expressing human red cone pigment in *Xenopus* rods (38). Since mammals use A1 chromophore, A1 red cone pigment is perhaps 40-fold less prone to spontaneous isomerization than the A2 form (40). This is likely due to the fact that the A2 chromophore has an additional double bond in the  $\beta$ -ionone ring, which has been suggested to lower the energy barrier for isomerization (44). Consequently, this introduces

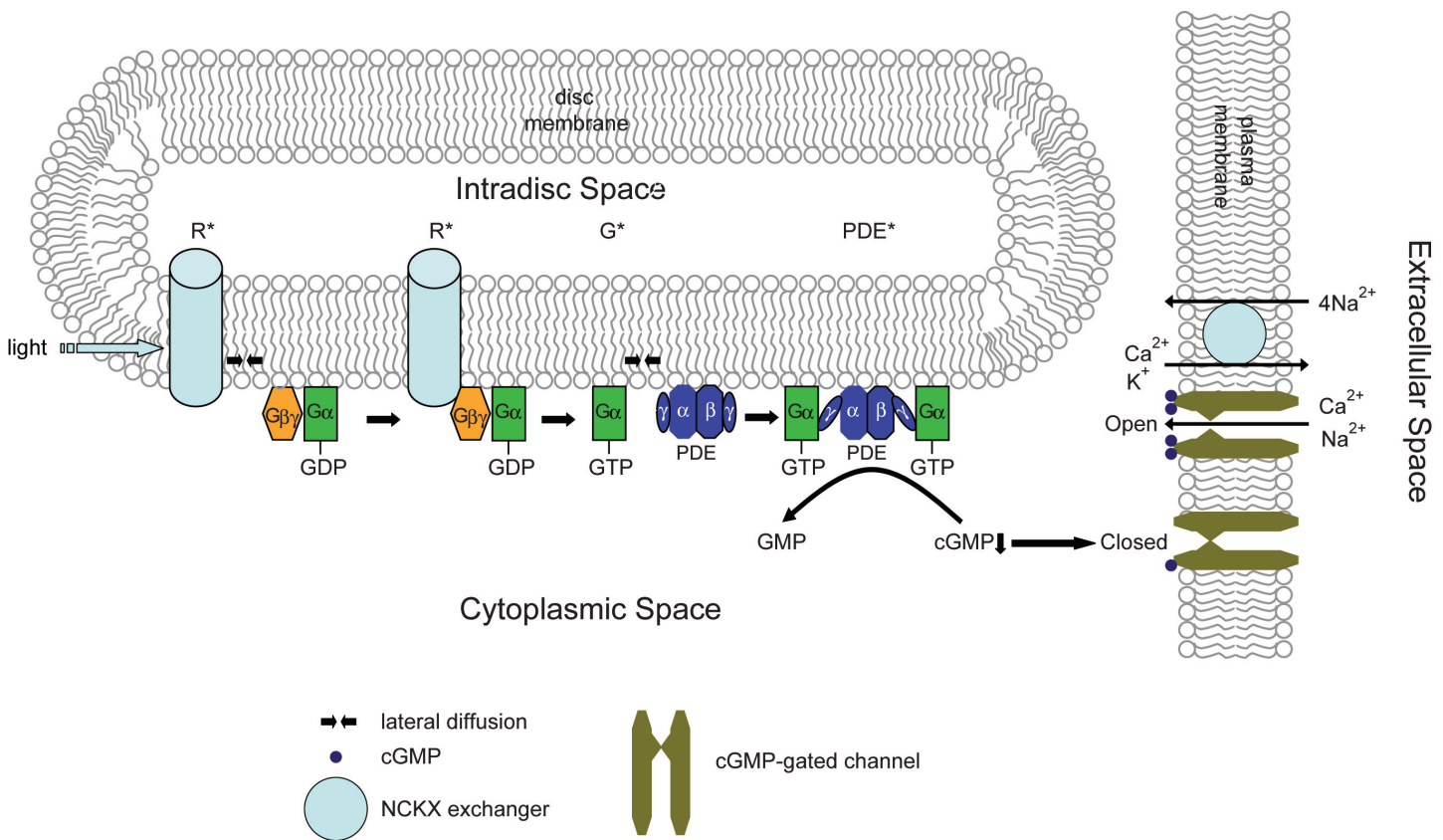


Figure 7. Schematic representation on the activation of vertebrate rod phototransduction. Following photon absorption, the activated rhodopsin ( $R^*$ ) activates the heterotrimeric G protein, catalyzing the exchange of GDP for GTP, producing the active  $G\alpha^*$ -GTP. Two  $G\alpha^*$ -GTP bind to the two inhibitory (subunits of PDE, thereby releasing the inhibition on the catalytic  $\alpha$  and  $\beta$  subunits, forming PDE\*, which in turn catalyzes the hydrolysis of cGMP. The consequent decrease in the cytoplasmic free cGMP concentration leads to the closure of the cGMP-gated channels on the plasma membrane and blockage of the influx of cations into the outer segment, which results in the reduction of the circulating dark current.

a red shift in absorption (45) and decreases the thermal stability of the A2 pigment. Incidentally, A1 rhodopsin was found to be 30 times more stable than A2 rhodopsin, rather similar to the finding for red cone pigment (46). More importantly, unlike in lower vertebrates such as salamander where A2 red cone pigment is sufficiently noisy as to impose a potential adaptational influence on cones even in darkness (38, 39, 47), A1 red cone pigment (and likewise for green and blue cone pigments) in primates and presumably other mammals should be quiet enough to have hardly any adaptational influence on cone sensitivity. In other words, the much lower absolute sensitivity of mammalian cones compared to mammalian rods appears to arise not from quantal noise in the pigments themselves, but from other phototransduction steps (48-50). This may explain why primate red, green and blue cones, unlike their amphibian counterparts (51, 52), all have similar sensitivities irrespective of their difference in visual pigments (41).

Photon absorption by 11-*cis*-retinal triggers the *cis*-to-*trans* isomerization of the retinoid chromophore (53, 54). As early as in the 1930s-1950s, vision scientists knew that rhodopsin bleaches in stages over intermediates that were short-lived at room temperature, yet stable at low temperatures (55-57), (Figure 10). Hubbard and Kropf measured the "bleaching intermediates (a mixture of lumirhodopsin and metarhodopsin)" by spectrophotometry at  $-17^\circ\text{C}$  (58). Photo-isomerization rapidly converts the ligand from a powerful inverse agonist to a powerful agonist, leading to the formation of a series of spectrally distinct intermediates of rhodopsin in the order of bathorhodopsin, lumirhodopsin, metarhodopsin I (Meta I), and metarhodopsin II (Meta II) within a few millisecond (Figure 10) (reviewed in Okada and Palczewski, 2001 (59)). Meta II is the active form of rhodopsin ( $R^*$ ), which in turn decays to the inactive Meta III. The Meta-II state of cone pigment

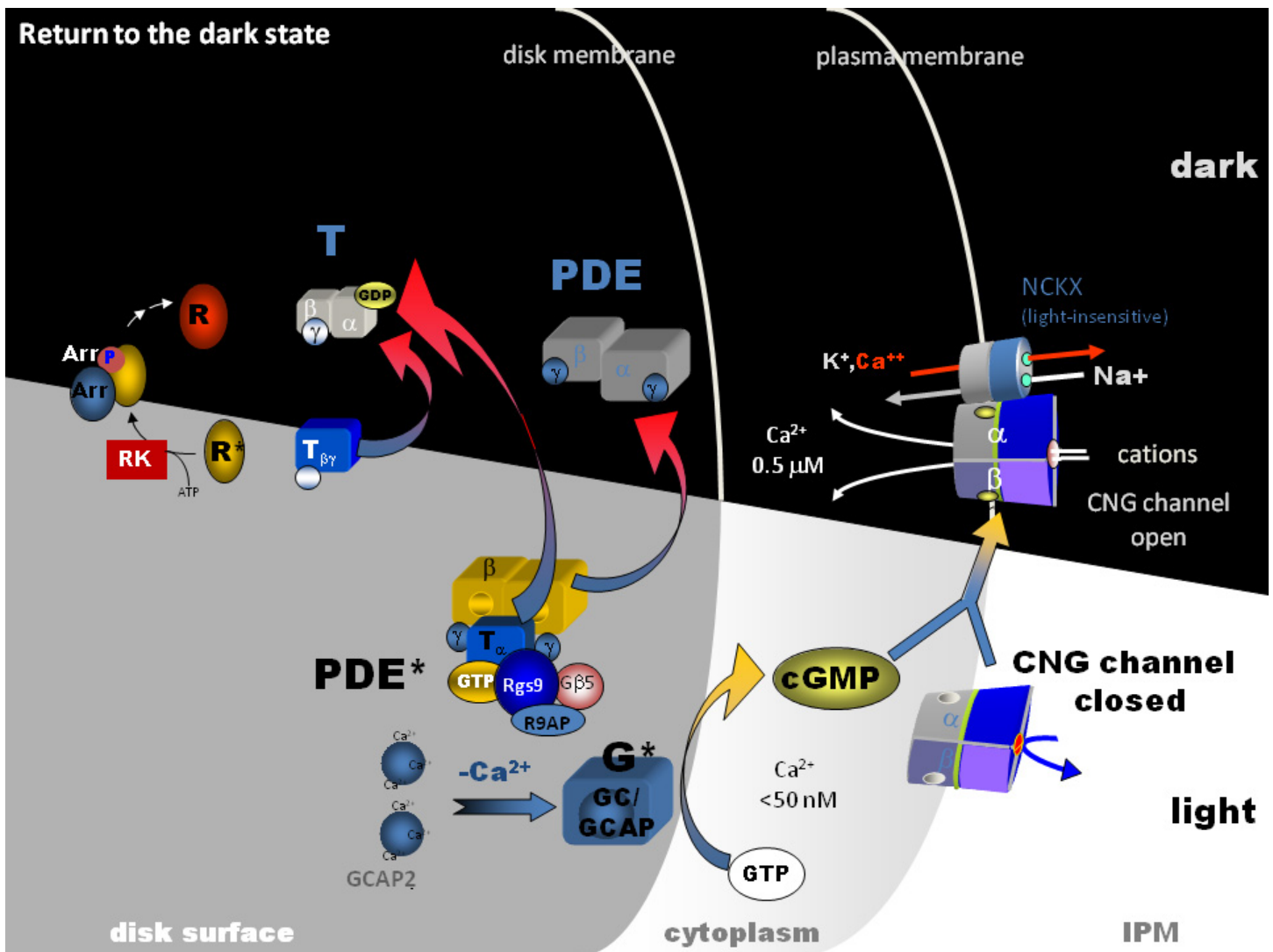


Figure 8. Recovery of rod phototransduction cascade that results in the re-opening of cGMP-gated channels on the plasma membrane (from light to dark state). IPM, interphotoreceptor matrix; R, rhodopsin (inactive); R\*, rhodopsin (active); T, transducin; PDE, phosphodiesterase (inactive); PDE\*, phosphodiesterase (active); Rgs9, regulator-of-G-protein-signaling protein 9; R9AP, RGS9 anchor protein; GC, guanylate-cyclase; NCKX, Na/Ca,K exchanger; Arr, arrestin; GCAP, guanylate-cyclase-activating protein. Courtesy of Wolfgang Baehr.

decays 50 times more rapidly than that of rhodopsin (60-62). Despite this difference, rhodopsin and transgenic red cone cone pigment, and vice versa, signal identically downstream when compared side-by-side in the same *Xenopus* rod or cone (38). The same was found for rhodopsin and transgenic red cone pigment in mouse rod (40). Thus, not only do rod and cone pigments interact with a given transducin, pigment kinase and arrestin in quantitatively identical ways, but the shutoff mediated by pigment kinase and arrestin also precedes the Meta-II decay of rod and cone pigments, rendering the decay of Meta II non-rate-limiting under normal conditions (see R\* termination).

Retinal absorbs maximally in the UV-range (max  $\sim 380$  nm) when in solution or bound to opsin in the unprotonated form. The absorption shifts into the visible region when the Schiff-base (SB) is protonated. Like other vertebrate pigments, mouse rhodopsin and M-cone pigment are protonated. On the other hand, mouse S-cone pigment is unprotonated, explaining its absorption in the UV-region (63). The positively charged Schiff-base is stabilized by the counterion E113 (residue number according to mouse rhodopsin) in rhodopsin and M-cone pigment (21, 64-66). Rhodopsin activation involves a "counterion switch" mechanism in which E181

located in the extracellular loop II transfers a proton via a hydrogen-bonded network to the primary counterion, E113, during the formation of Meta I. Therefore, E181 replaces E113 as the counterion to stabilize the protonated Schiff-base in the transition stage before its eventual deprotonation ((67), Figure 11).

Because the mouse S-cone pigment is not protonated and the nearby E113 is neutral, the interesting questions are: does a protonation event occur during light activation, and does it involve a "counterion switch" mechanism? Remarkably, after the 11-cis isomerization, the Schiff-base picked up a proton in the Lumi state from E108 to become transiently protonated (68) and a counterion switch occurs from E108 (E113 in rhodopsin) to E176 (E181 in rhodopsin) during the Lumi to Meta I transition, in close analogy to rhodopsin ((69), Figure 12). The photoactivation mechanism of S-cone pigment, SB → PSB (protonated Schiff-base) (+):E108(-) → PSB(+):E176(-) → SB, makes vision possible in the UV region. Thus, the counterion switch appears to be a general mechanism for the activation of all visual pigments.

The decay of R\* eventually leads to the departure of all-trans-retinal from the protein. The all-trans chromophore is converted back to 11-cis-retinal through a cascade of enzymatic reactions called the visual cycle in the adjacent RPE, before being used again for the regeneration of visual pigments (for example, see review McBee et al., 2001 (70)).

Visual pigment is a major structural component of rods and cones. It is not surprising that genetic deletion of mouse rhodopsin results in rods without proper outer-segment formation (3, 4). Is half the amount of normal rhodopsin enough for maintaining a healthy ROS? In rho<sup>+/-</sup> mouse, rods are properly formed despite only half of the normal level of rhodopsin being present. However, a progressive mild degeneration of the rods does occur. Interestingly, the activation rate of the photoresponse of rho<sup>+/-</sup> rods is twice that of normal (71). The explanation for this observation was originally proposed that a lower rhodopsin concentration reduces protein crowding on the disc membrane, thereby increasing rhodopsin's diffusion coefficient and its rate of encounter with transducin. This finding thus would point to the diffusional encounter of transducin by photoexcited rhodopsin as the rate-limiting step in the activation of the rod photoresponse. However, Liang et al. subsequently reported that rods in rho<sup>+/-</sup> mouse are not completely normal in that rhodopsin exists in small raft-like structures as well as in large and organized para-crystals (72). In addition, there is an approximate 40% reduction in the ROS volume, in the rhodopsin content and in the 11-cis-retinal level in these cells. These authors suggested that the observed acceleration of phototransduction in rho<sup>+/-</sup> rods was not due to a lower density of rhodopsin on the disc surface but to the structural changes in the whole ROS.

## 8. High quantum efficiency of photoactivation

The quantum efficiency of photoactivation measures the probability that the adsorption of a photon initiates photoactivation. This probability is defined as the ratio between the number of photoactivated molecules and the number of molecules that absorbed a photon. Quantum efficiency of visual pigments is wavelength-independent at ~ 0.7 in the spectrum of visible light whereas it falls to about 0.25 for wavelengths shorter than 300 nm (73). This suggests that every absorbed photon in the visible range can activate rhodopsin equally well. The quantum efficiency of 0.7 is very similar across all visual pigments. This high efficiency seems to be a common feature of most vertebrate visual pigments.

## 9. The activation of transducin constitutes the first amplification step

Photoactivated pigment binds the transducin heterotrimer and catalyzes the exchange of GTP for GDP on the α-subunit. Gα-GTP (G\*) dissociates from R\* as well as its native partners, Gβγ and interacts with the cGMP phosphodiesterase (PDE) to carry the signal forward. Released R\* is free to activate additional transducin molecules. Transducin activation by R\* represents the first amplification step in the phototransduction cascade.

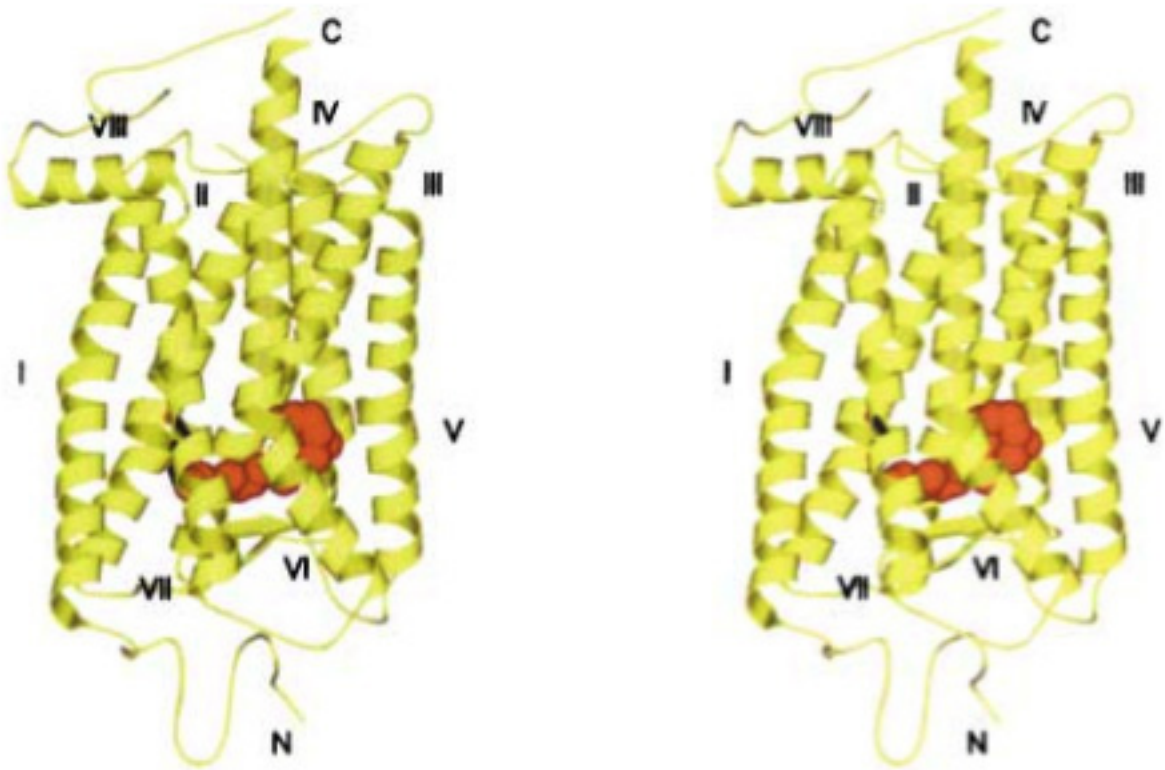


Figure 9a Stereo pair of the crystal structure of rhodopsin. From Stenkamp et al. 2002 (209).

The estimated rate of transducin activation by a single  $R^*$  has ranged from 10 to over  $3000\text{ s}^{-1}$  at room temperature (for review see Pugh and Lamb, 1993). More recently, a rate of  $\sim 120\text{ s}^{-1}$  was reported to be more consistent with biochemical, light-scattering, and electrophysiological measurements ((74), but see (75)). The rate is roughly doubled in mammalian rods due to a difference in body temperature. Until recently, it was believed that over a hundred transducins are activated during the lifetime of a single  $R^*$  in mammalian rods (76). This number is now revised to be  $\sim 20$  in mouse rods, based on the shorter life time of  $R^*$  (80 msec) and  $240\text{ s}^{-1}$  activation rate of transducin by  $R^*$  (77).

Transducin is present at 10% the amount of pigment. Rods and cones have different isoforms of transducin, being  $G\alpha_1G\beta_1\gamma_1$  in rods and  $G\alpha_2G\beta_3\gamma_8$  in cones (78-81). The C-terminal of the  $\gamma$  subunit is farnesylated and the N-terminal of the  $\alpha$  subunit is acylated (82-84). These lipid modifications help anchor the holo-transducin to the disc membrane. The importance of transducin for conveying the signal from  $R^*$  to PDE was confirmed by gene-targeting experiments, in which rods of  $G\alpha_1$ -null mice ( $gnat1^{-/-}$ ) were found to lose all light sensitivity (85). The  $gnat1^{-/-}$  mouse line has proven to be a valuable tool for blocking rod phototransduction in many studies (86-88). It was also used successfully to delineate two apoptotic pathways in light-induced retinal degeneration (89). Bright light triggers apoptosis of photoreceptors through a mechanism requiring the activation of rhodopsin but not transducin signaling. In contrast, low-intensity light induces apoptosis that is predominantly dependent on transducin signaling.

Almost two decades ago, rod transducin was found to undergo light-dependent redistribution (164, 219). Great progress has been made in the past few years by using mouse (or rat) models for study. Both  $G\alpha_2$  and  $G\beta_1\gamma_1$  subunits are present predominantly in the ROS in darkness, but translocate in bright light, with slightly different time courses, to the inner segment and the inner nuclear layer (90). This phenomenon has been suggested to contribute to light adaptation of rods (91), but others argue that the main function of transducin translocation is to provide protection for rods in bright light when rods contribute little to vision (92). In contrast,  $G\alpha_2$  has been

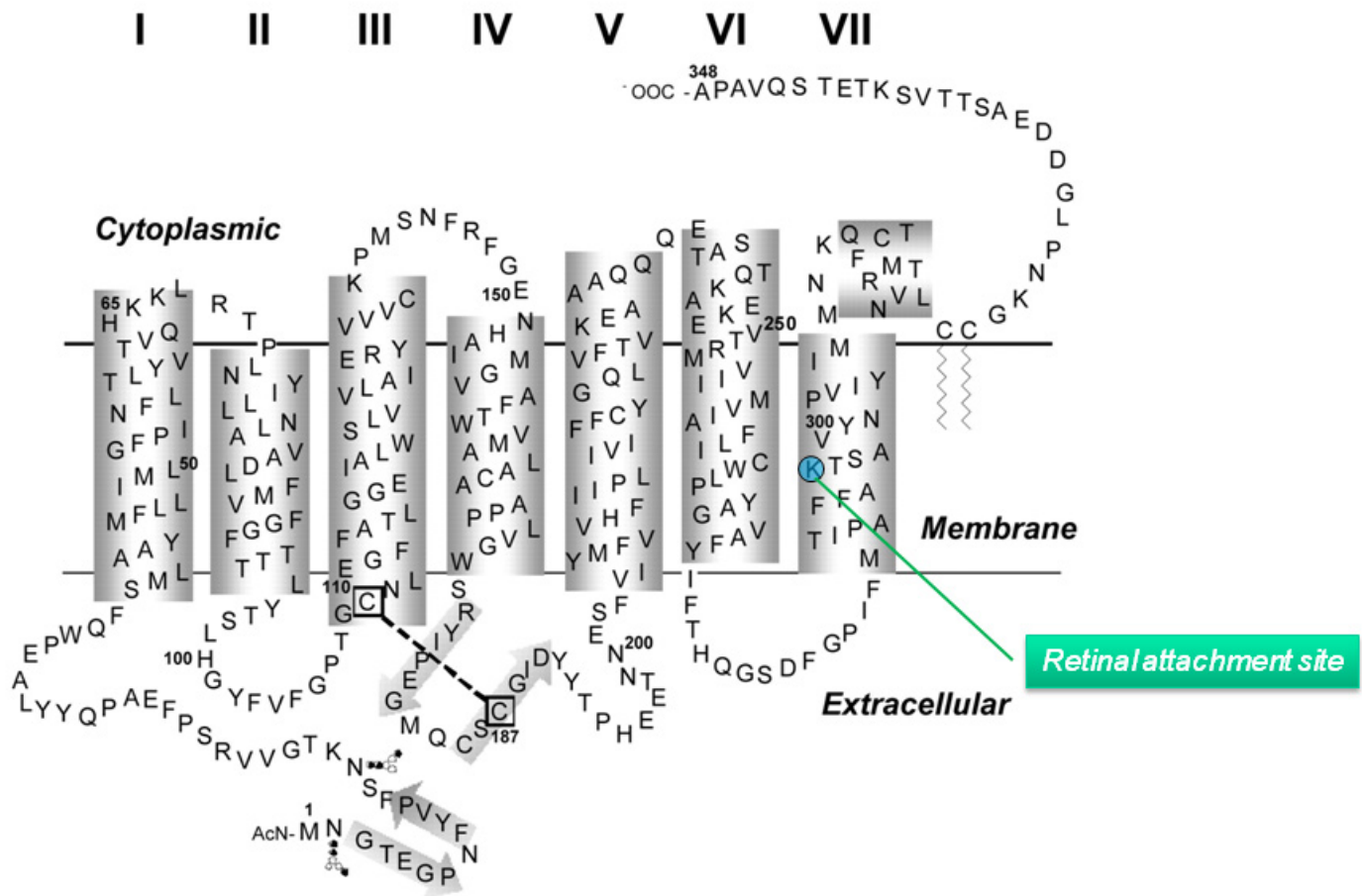


Figure 9b. Structural model of bovine rhodopsin showing seven transmembrane components and the attachment site for retinal. The seven-TM helices are shown by numbered gray boxes, and  $\beta$ -strands are shown by arrows. The respective residue ranges of these TM helices are as follows: I, 35-60; II, 71-100; III, 107-137; IV, 151-173; V, 200-225; VI, 247-277; VII, 286-306; VIII, 310-324. The dashed line indicates the C110-C187 disulfide bond located at the interface between the TM and EC domains. Reprinted from (208)

found not to translocate from the cone outer segment (COS) in light under physiological conditions (92-94) and only translocates away from the cone outer segment under very high-intensity light (95). This might be consistent with the need for cones to function in bright light (92).

$G_{\gamma 1}$  in rods and  $G_{\gamma 8}$  in cones are farnesylated with a 15-carbon chain, but all other  $G_{\gamma}$  subunits are geranylgeranylated with a 20-carbon chain. What is the significance of this difference? Knock-in mice expressing geranylgeranylated instead of farnesylated  $G_{\gamma 1}$  exhibited impaired properties in light adaptation because the stronger attachment by geranylgeranylation attenuated the light-dependent translocation of  $G_{\gamma 1}$  from ROS to the inner region (90). It thus appears that the selective farnesylation is important for the regulation of visual sensitivity by providing sufficient but not excessive anchoring of  $G\beta_{1\gamma 1}$  to the membrane.

## 10. The high catalytic power of PDE accounts for the second amplification step

PDE is the third component of vertebrate phototransduction. It is a tetrameric protein consisting of two equally active catalytic subunits,  $\alpha$  and  $\beta$ , and two identical  $\nu$  subunits (96-98). PDE is anchored to the disc membrane by isoprenylation of the C-termini of the two catalytic subunits (99, 100). The density of PDE is  $\sim 1$ -2% of rhodopsin. Thus, the first three components of phototransduction are present in the ratio of 100R:10G:1PDE.

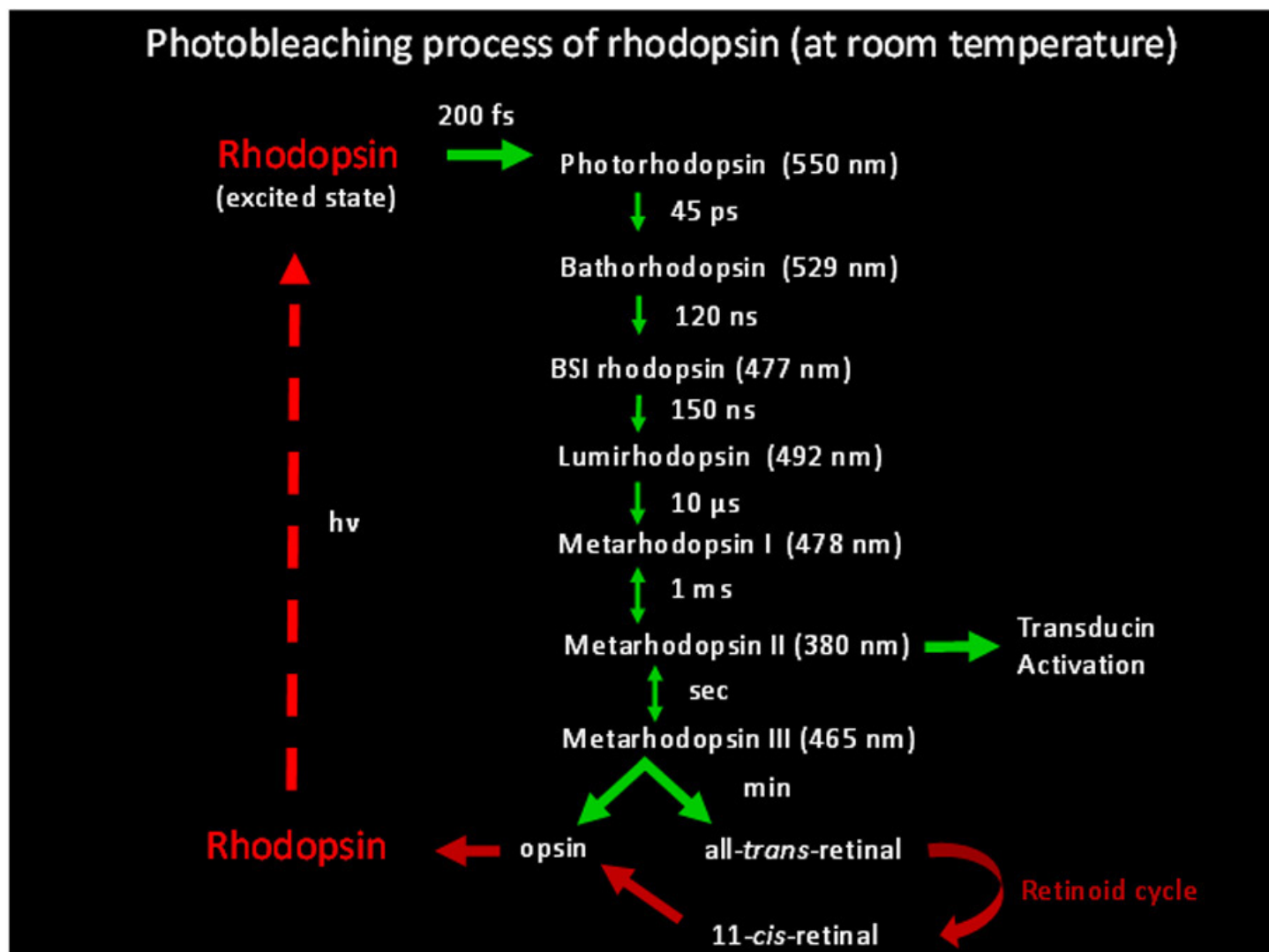


Figure 10. Photobleaching process of bovine rhodopsin. After photon absorption and electronic excitation, fast isomerization of the chromophore leads to the formation of a series of intermediate states of rhodopsin. This is called the "bleaching process" because rhodopsin loses its color. The intermediate states were identified by both low-temperature and time-resolved spectroscopy. The peak spectral sensitivity of each state was indicated. BSI, blue-shifted intermediate. Modified from Wolfgang Baehr.

In the dark, the two  $\gamma$  subunits act as inhibitory subunits by binding to the two catalytic subunits. In the light,  $G\alpha$ -GTP encounters PDE $\gamma$  and sterically displaces the latter (still associated with PDE $\alpha\beta$ , therefore relieving its inhibitory effect on the catalytic subunits and permitting the hydrolysis of cGMP to proceed.

In contrast to the amplification achieved during transducin activation by  $R^*$ , the activation of PDE by  $G^*$  constitutes no gain, i.e. with an efficiency approaching at most unity. It is the catalytic power of PDE $^*$  that provides the second amplification step. It was reported that PDE $^*$  hydrolyzes cGMP at a rate close to the limit set by aqueous diffusion, with a  $K_m$  of  $\sim 10 \mu\text{M}$  and a  $K_{cat}$  of  $2200 \text{ s}^{-1}$  (74, 96). The combined amplification provided by rhodopsin and PDE are very high ( $\sim 10^5$ - $10^6$ ), ensuring the high sensitivity of rods, including the ability of rods to detect single photons (for review see (19, 101)).

One might have expected that the deletion of PDE $\gamma$  from mouse rods would unleash the full catalytic power of PDE $\alpha\beta$ . However, Tsang et al. found that, in the absence of PDE $\gamma$ , the PDE $\alpha\beta$  dimer actually lacked hydrolytic activity, and the photoreceptors of the mutant mouse rapidly degenerated (102). Thus, the inhibitory PDE $\gamma$  subunit appears to be necessary for the integrity of the catalytic PDE $\alpha\beta$  subunits. The degeneration might be caused by an abnormally high cGMP concentration due to the lack of hydrolysis. A related example is the rd



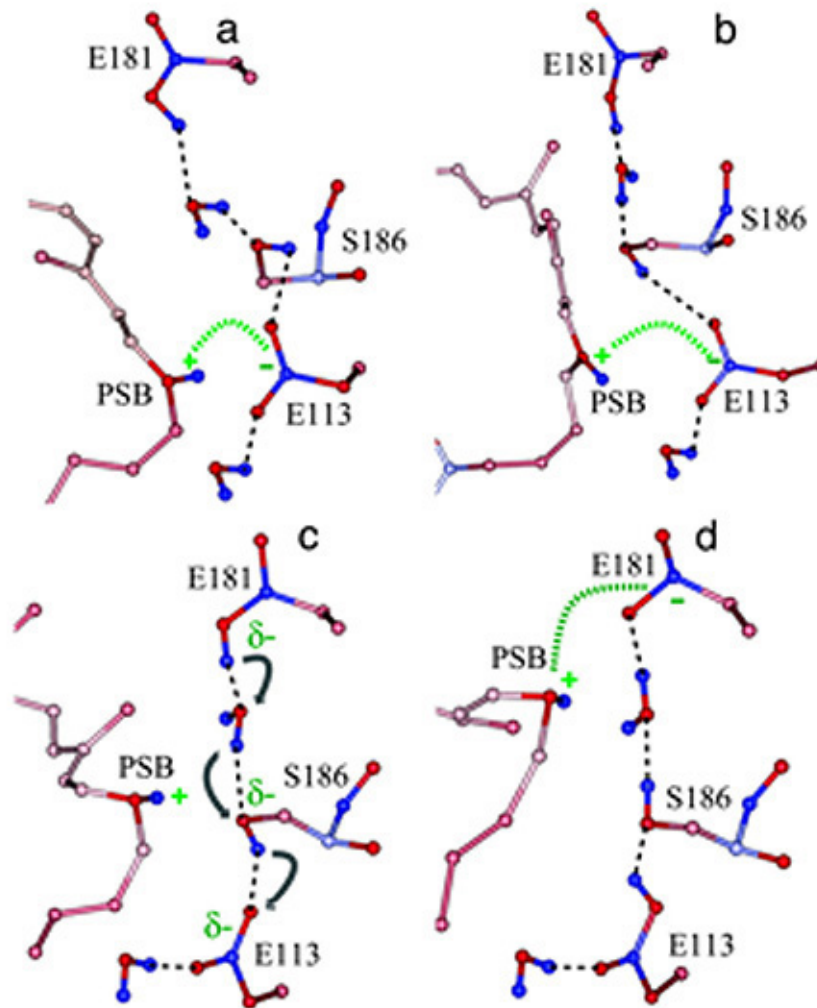


Figure 11. Schematic of the proposed proton transfer mechanism for switching the protonated Schiff-base (PSB) counterion in rhodopsin. (a) Rhodopsin: two water molecules and Ser-186 form a H-bond chain between Glu-113 and Glu-181. Electrostatic interaction between the PSB and Glu-113 is indicated by the green dashed line. (b) Blue-shifted intermediate: after photoisomerization, the H-bond chain evolves so that the two water molecules and Ser-186 are lined up to prepare for the proton transfer and the PSB has shifted relative to Glu-113. (c) Lumirhodopsin: the PSB shifts further away from Glu-113 toward Glu-181. The gray arrows indicate a possible proton transfer pathway. (d) Metarhodopsin I: proton transfer is completed. The PSB group is now close to Glu-181 to establish the electrostatic interaction (green dashed line) with the new counterion. Reprinted from Yan et al., 2003 (67).

mouse, which is one of the best-known models for retinal degeneration. The rod cells in the rd mouse begin to degenerate at about P8, followed by cones; by 4 weeks, virtually no photoreceptors are left (103, 104). Degeneration in this mouse model is preceded by the accumulation of cGMP in the retina, correlated with deficient activity of the rod PDE due to a mutation in the  $\beta$  subunit (105, 106). It is worth noting that the rd mouse was instrumental in suggesting that inner retinal neurons could mediate non-image-forming vision (107, 108).

In addition to its inhibitory function, PDE $\gamma$  accelerates the GAP (GTPase Activating Protein) activity of  $G^*$  for self-shutoff (see  $G^*$ -PDE $^*$  termination). Mouse rods carrying the W70A point mutation of PDE $\gamma$  which impairs the  $Gat_1$ -PDE $\gamma$  interaction, showed a greatly reduced sensitivity to light and a slower recovery from the flash response than wild type (109).

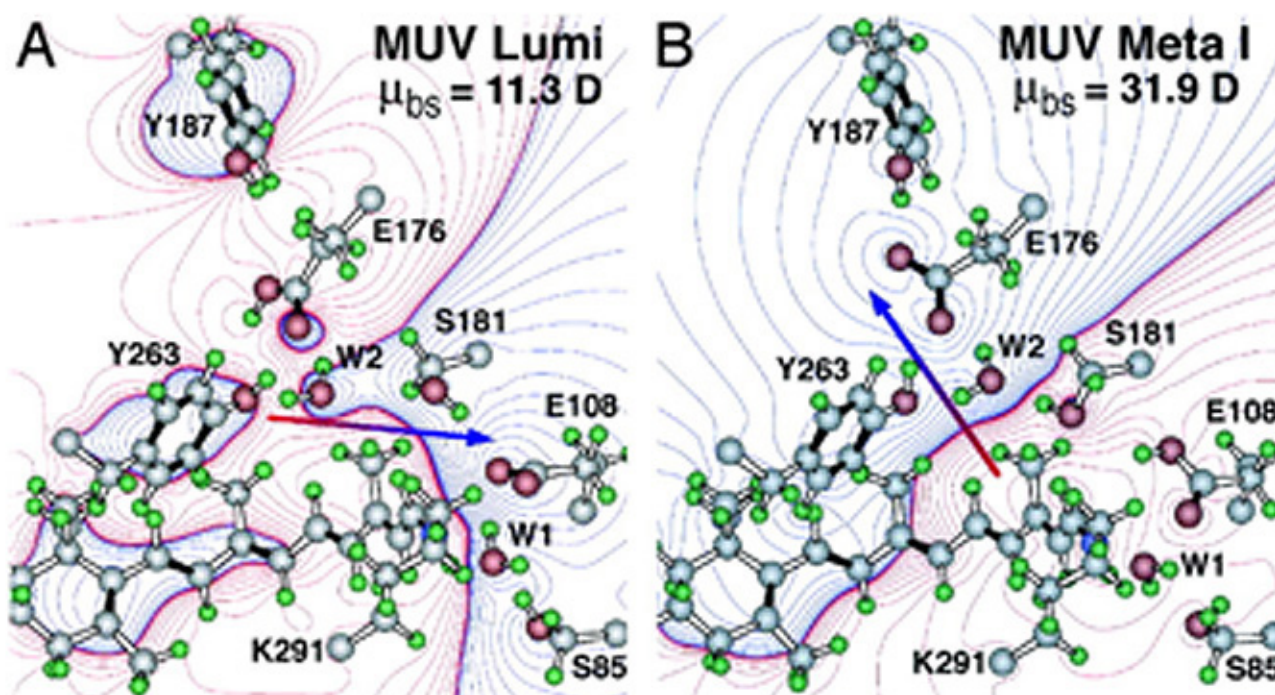


Figure 12. Molecular models of the lumi (A) and meta I (B) intermediates of mouse S-cone (UV) pigment based on the assumption that a counterion switch occurs during the lumi (E108 counterion) to meta I (E176 counterion) transformation. The dipole moments of the binding site residues,  $\mu_{bs}$ , are given in the upper right of A and B and the dipole moment vector is shown by using red-to-blue arrows. Reprinted from Kusnetzow et al., 2004 (69).

## 11. cGMP is the second messenger mediating rod phototransduction

By 1970, scientists generally believed that a second messenger was required to mediate the rod photoresponse based on several lines of evidence. First, light absorption occurs on the rod disc membrane, whereas the light sensitive conductance is in the plasma membrane. Since rod discs are separate from the plasma membrane, a second messenger is required to connect the two. Second, the dim-flash response of rods lasts a few seconds, which is too long to be accounted by the open time of known membrane conductance. However, it took more than a decade before the identity of the second messenger was finally determined to be cGMP (reviewed in (110)). The "fierce battle was fought" on the validity between two competing candidates,  $\text{Ca}^{2+}$  and cGMP. According to the  $\text{Ca}^{2+}$  hypothesis, which was first proposed by Hagins (6), the concentration of intracellular free  $\text{Ca}^{2+}$  is low in the dark and rises in the light to block light-sensitive current. The main supporting evidence was that reducing the concentration of external  $\text{Ca}^{2+}$  dramatically increases the dark current, suggesting internal  $\text{Ca}^{2+}$  inhibits the dark current. On the other hand, the cGMP hypothesis proposed that the concentration of cGMP was high in the dark to maintain a cGMP-dependent conductance. Light led to the hydrolysis of cGMP and the subsequent closing of the conductance. The supporting evidence is that intracellular injection of cGMP increases the amplitude and latency of the photoresponse. Adding to the complexity is the finding that the free cGMP concentration varies inversely with the free  $\text{Ca}^{2+}$  concentration in rods, making it difficult to separate the effect of the two.

This debate was finally settled with the discovery of cGMP-gated channels in rods by Fesenko and colleagues in 1985 (111). By using the patch-clamp technique, they showed that cGMP increased a cation conductance of

inside-out patches of outer-segment plasma membrane without the need of ATP. The direct channel gating by cGMP is surprising because cyclic nucleotides were generally believed to act through cyclic-nucleotide dependent kinases and protein phosphorylation on target proteins at that time. This dogma partially explained scientists' reluctance to embrace the cGMP hypothesis because protein phosphorylation was too slow. Another monumental work by Yau and Nakatani was published at the same year that helped the anointment of cGMP as the right candidate (112). An identical cGMP-gated cation conductance was found on a truncated rod outer segment with an intact plasma membrane. Most importantly, this conductance could be suppressed by light, suggesting that the long-sought light-sensitive conductance is the cGMP-gated conductance. The publications by Fesenko and Yau marked the end of the  $\text{Ca}^{2+}$  hypothesis.

## 12. The cGMP-gated channel provides the final step of photo-activation

The cGMP-gated channel belongs to the family of cyclic-nucleotide-gated (CNG) channels, which are non-selective cation channels (reviewed in (113, 114)). The channel is located on the plasma membrane and is the last component in the activation phase of phototransduction. In the dark, a basal concentration of one to several  $\mu\text{M}$  cGMP keeps a small percentage of the CNG channels open (115). The decline in cGMP concentration upon illumination leads to rapid closure of the channels with a sub-millisecond delay (116). The gating of the rod channel by cGMP is cooperative with a Hill coefficient of  $\sim 3$ ; therefore, the light-triggered suppression of the dark current is 3 times larger than the decrease in the intracellular cGMP concentration.

For a long time, the rod channel was believed to be a hetero-tetramer consisting of 2 CNGA1 and 2 CNGB1 subunits. In 2002, a number of laboratories made the surprising discovery that the rod channel actually has a 3CNGA1:1CNGB1 subunit composition (117-119), whereas the cone channel supposedly exhibits a 2CNGA3:2CNGB3 stoichiometry (120). CNGA1 and CNGA3 subunits form functional homomeric channels by themselves when heterologously expressed. Although CNGB1 and CNGB3 do not form functional channels by themselves, they confer several properties typical of native channels when co-expressed with A subunits: flickery opening behavior, increased sensitivity to L-cis-diltiazem (a CNG channel-specific inhibitor), and weaker block by extracellular calcium (113, 121-123).

In humans, mutations in CNGA1 causes retinitis pigmentosa (124), while mutations in both CNGA3 (125) and CNGB3 (126) cause achromatopsia. Mouse models carrying null mutations of CNGB1 (127) and CNGA3 (121) are available. CNGB1 was found to be crucial for the targeting of the native CNG channel in rods. Thus, only trace amounts of the CNGA1 subunit were found on the ROS in CNGB1-null mice and the majority of rod photoreceptors failed to respond to light (127). CNGA3-deficient mice selectively lost their cone photoresponse with the rod pathway intact. Analogous to the case of rod transducin, CNGA3-null mice were used to block cone phototransduction in studying the intrinsically photosensitive retinal ganglion cells (86, 87).

In the dark, the concentration of free cGMP in the rod outer segment was estimated to be several  $\mu\text{M}$ , which is lower than the  $K_{1/2}$  ( $\sim 10$ - $40 \mu\text{M}$  depending on  $\text{Ca}^{2+}$  concentration), the concentration of cGMP necessary to half-maximally activate the channel. As a result, only  $\sim 1\%$  of the CNG channels are open! In other words, 99% of the channels are already closed in the dark and light can only suppress the remaining 1% channels. This explains why current induced by cGMP injection is more than 10 times larger than the dark current.

The inward current through the cGMP-gated channel is composed of  $\sim 85\%$   $\text{Na}^+$  because  $\text{Na}^+$  is the predominant external cation and the channel is non-selective to monovalent cations. The remaining current is mainly carried by  $\text{Ca}^{2+}$  with a minor contribution from  $\text{Mg}^{2+}$  (115, 128). Extracellular  $\text{Ca}^{2+}$  actually partially blocks the channel to reduce its conductance under physiological conditions. The inward current is balanced by an outward current flowing across the inner-segment membrane, which is mainly carried by potassium ions. This "circulating current" is also called "dark current" in both rods and cones (6). Unlike other ligand-gated

channels, the CNG channel does not desensitize to cGMP, which is important for rods to maintain a steady dark current ranging between 20 and 70 pA in vertebrate rods. The rod photoresponse is essentially a transient suppression of the circulating current. It was estimated that the dark current was carried by ~ 10, 000 channels. The participation of large numbers of "micro" channels averages out the channels noise, i.e. reduce an otherwise substantial stochastic channel noise if the dark current were carried out by a few "macro" channels. This feature improves the sensitivity of rods.

Two extrusion mechanisms are critical to maintain ionic balance in rods. An energy-dependent Na-K ATPase at the inner segment pumped  $\text{Na}^+$  out and  $\text{K}^+$  into the cells. A Na/Ca,K exchanger (NCKX) in the outer-segment plasma membrane extrudes one  $\text{Ca}^{2+}$  and one  $\text{K}^+$  outward in exchange for four  $\text{Na}^+$  inward producing the net entry of one positive charge. The exchanger and the CNG channel were found to form a stable complex on the plasma membrane, likely as a way to control the stoichiometry between the two, which is critical for regulating  $\text{Ca}^{2+}$  concentration in the rod outer segment. During the light response, the influx of  $\text{Ca}^{2+}$  is reduced due to the closure of some CNG channels while the efflux of  $\text{Ca}^{2+}$  through the exchanger is maintained. The resulting  $\text{Ca}^{2+}$  decline triggers negative feedback to produce light adaptation.

### 13. Phototransduction termination

Following light activation, a timely recovery of the photoreceptor is essential so that it can respond to subsequently absorbed photons, and signal rapid changes in illumination. This recovery from light requires the efficient inactivation of each of the activated components:  $\text{R}^*$ ,  $\text{G}^*$ , and  $\text{PDE}^*$ , as well as a rapid restoration of the cGMP concentration. The termination rates of the activation steps set the time course of the photoresponse.

In the past decade, knowledge gained from genetically engineered mouse lines has provided major advances in understanding the termination of the rod photoresponse. In the following sections, we shall discuss separately the events responsible for the inactivations of  $\text{R}^*$ ,  $\text{G}^*$  and  $\text{PDE}^*$ , followed by the restoration of cGMP.

### 14. $\text{R}^*$ termination

Activated rhodopsin ( $\text{R}^*$ ) is inactivated by a two-step process. First,  $\text{R}^*$  is phosphorylated by rhodopsin kinase (GRK1), which lowers the activity of  $\text{R}^*$ . Second, the protein arrestin (Arr1) binds to phosphorylated  $\text{R}^*$ , capping its residual activity (129, 130).

Multiple serine/threonine residues at the C-terminal of rhodopsin (six in mice and seven in humans) provide the phosphorylation sites for GRK1. Cone pigments have more potential phosphorylation sites at the C-terminal than rhodopsin. For example, human red cone pigment has 10 such sites. Even though biochemical experiments originally suggested that rhodopsin is predominantly phosphorylated at only one serine residue following light exposure (131), subsequent recordings from transgenic mouse rods carrying phosphorylation-site mutations suggested that the reproducible deactivation of  $\text{R}^*$  requires at least three phosphorylation events (132). In addition, all six sites need to be phosphorylated in order for the normal decline of the response to proceed.

Multiple phosphorylation events are also proposed to underlie the reproducibility of rod responses to single-photons (132-134). Despite the fact that events generated by single molecules are stochastic in nature, the single-photon response of rods shows remarkable reproducibility in amplitude and shape (15, 135, 136). By averaging over multiple shutoff steps, the integrated  $\text{R}^*$  activity varies less than otherwise controlled by a single step. This hypothesis is supported by experiments using transgenic mouse rods carrying phosphorylation-site mutations (137). The authors showed that the reproducibility of the single-photon response varies in a graded and systematic manner with the number, but not the identity, of the phosphorylation sites. Each phosphorylation site provides an independent step in rhodopsin deactivation and that, collectively, these steps tightly control the lifetime of  $\text{R}^*$ .

Much less is known about the role of the phosphorylation sites in cone pigments. The only *in vivo* experiment was done by Kefalov et al. (38), showing that transgenic frog rods expressing a human red cone pigment with all 10 putative phosphorylation sites mutated gave a prolonged response. It suggests that activated cone pigment is quenched by a similar two-step shutoff mechanism even though its active lifetime is much shorter than that of rhodopsin.

In addition to mutations of all of the C-terminal serine and threonine residues to alanine (132), rhodopsin phosphorylation can also be prevented by deleting the C-terminal region of the pigment (138) or ablating GRK1 (139). As expected, rods from all three transgenic mouse lines showed similar properties of the single-photon response, with an amplitude reaching a plateau about twice that of wild-type and decaying stochastically to baseline after a long interval of 3 to 5 seconds. GRK1-mediated phosphorylation begins to reduce the activity of  $R^*$  at ~100 msec after the flash, because this is the time point at which the transgenic response starts to deviate from the WT response (Figure 13). As mentioned earlier, it was estimated in a recent study that the lifetime of  $R^*$  is ~80 msec (77), suggesting that arrestin binding occurs rapidly after phosphorylation of the pigment. Therefore, GRK1/arrestin mediated shutoff occurs in rods even earlier than the fast Meta-II decay of cone pigment (38), which is of the order of 1 s after flash (60, 62, 140). The GRK1-mediated shutoff likely happens even faster in cones (see below).

Mouse and rat are unusual in that the same GRK1 is present in both rods and cones. In all other species studied, another pigment kinase (the so called "cone pigment kinase"), GRK7, is present in cone photoreceptors (141-144). Indeed, many animal species, including human, have both GRK1 and GRK7 in cones. This explains why Oguchi patients with a defective GRK1 gene have normal daytime vision whereas GRK1-null mice have prolonged cone photoresponses (145, 146). Interestingly, GRK7 was shown to have considerably higher specific activity than GRK1 and, in fish, is present at a much higher concentration in cones than GRK1 is in rods (142, 147). This difference has been proposed as a potential mechanism underlying the faster shutoff and lower sensitivity of cones than rods (reviewed in (148)).

Biochemical experiments suggest that GRK1-mediated phosphorylation of  $R^*$  is regulated by recoverin (Rec) (149-152), which belongs to a family of calcium-binding proteins. The hypothesis is that, when intracellular free  $Ca^{2+}$  concentration is high in the dark, Rec- $Ca^{2+}$  binds to GRK1 and inhibits  $R^*$  phosphorylation. When  $Ca^{2+}$  concentration decreases in the light,  $Ca^{2+}$  dissociates from recoverin; consequently, the resulting affinity between recoverin and GRK1 is reduced, and its inhibition on  $R^*$  phosphorylation is released. However, this hypothesis was challenged by *in vitro* measurements suggesting that the extent of  $R^*$  phosphorylation was unaffected by light adaptation and by changes in intracellular  $Ca^{2+}$  (153). This controversy was finally settled by recordings from Rec<sup>-/-</sup> mouse rods (154), which showed that Rec- $Ca^{2+}$  prolongs the dark-adapted flash response and increases the rod's sensitivity to dim steady light, probably by inhibiting the phosphorylation of  $R^*$  by GRK1. Furthermore, Rec<sup>-/-</sup> rods had faster  $Ca^{2+}$  dynamics, indicating that recoverin is a significant  $Ca^{2+}$  buffer in the ROS.

In the second step for the deactivation of  $R^*$ , arrestin binds to phosphorylated  $R^*$  ( $R^*$ -P) to cap its catalytic activity. In mouse, the dim-flash responses from rods of arrestin-knockout (Arr<sup>-/-</sup>) mice do not differ greatly from the wild-type response until in its falling phase, when recovery reaches approximately halfway back to baseline (155). Therefore, phosphorylation alone can reduce  $R^*$ 's activity significantly. The response of Arr<sup>-/-</sup> rods on average recovers ~10 times more slowly than the response of rods lacking rhodopsin phosphorylation (Figure 13), presumably reflecting the continuous activity of the phosphorylated meta-II state of  $R^*$  until it decays to inactive meta III. In rods lacking both GRK1 and arrestin (GRK1<sup>-/-</sup>Arr<sup>-/-</sup>), the activation phase and peak amplitude of the dim-flash response resemble those of GRK1<sup>-/-</sup> rods but then decay slowly with a time constant similar to that of the Arr<sup>-/-</sup> response (156), reflecting the decay of non-phosphorylated R. It thus appears that phosphorylation does not influence the decay of  $R^*$ .

At least two splice variants exist for rod arrestin: a full-length (p48) and a C-terminal truncated form (p44) (157). P44 has a faster on-rate than p48 for binding  $R^*$  and  $R^*$ -P (158, 159). In addition, p44 is more efficient than p48 in turning off  $R^*$  in vitro (158, 160). Although p48 is ~10 times more abundant than p44, it translocates from ROS to the rest of the cell in the dark, therefore largely absent in dark-adapted ROS (161-164). This raises an interesting question about the roles of individual isoforms of arrestin in the intact rods. By selectively expressing the two isoforms in mouse rods lacking endogenous arrestin, it was found that both isoforms could quench the activity of phosphorylated  $R^*$  rapidly. However, only p48 was able to quench the activity of non-phosphorylated  $R^*$  (156).

Cones express their own arrestin called cone arrestin or X-arrestin (Arr4) (165, 166). Surprisingly, both the rod and cone forms of arrestin exist in mouse cones (167). Arr1 in cones is ~50-fold higher than that of Arr4 (168). Single cell recordings from cones of mice with one or both arrestins knocked out shows that arrestin is required for normal cone inactivation although removal of one arrestin has negligible effect (168).

## 15. $G^*$ -PDE $^*$ termination

Earlier, genetically engineered mouse lines were designed to disrupt  $R^*$  termination. More recent studies have centered on  $G^*$ -PDE $^*$  termination.  $G^*$  is inactivated when its bound GTP is hydrolyzed to GDP. Although transducin has a slow intrinsic GTPase activity, the hydrolysis is greatly accelerated by the GAP complex. The complex is composed of a member of the family of regulator-of-G-protein-signaling proteins (RGS9-1 (169), ), the long form of G $\beta$ 5 subunit (G $\beta$ 5-L (170), ), and a membrane-anchor protein (R9AP (171), ). RGS9-1 has a G protein  $\gamma$ -like (GGL) domain that binds to G $\beta$ 5-L, and has an N-terminal DEP (Dishevell/Eg110/Pleckstrin) domain that interacts with R9AP. After hydrolysis, G $\alpha$ -GDP dissociates from PDE $\gamma$  which allows the latter to re-exert its inhibition on the catalytic PDE $\alpha\beta$  subunits (reviewed in (76)). The molecular reactions underlying this step are shown schematically in Figure 14.

Even though only RGS9-1 has GAP activity, all three components of the GAP complex are obligatory partners because genetic ablation of any one of them in mouse resulted in an increased instability of the other two through a posttranscriptional mechanism (172-174). This is why transgenic mouse rods lacking RGS9-1, G $\beta$ 5-L, or R9AP display a similar delay in the recovery phase of the flash response without much noticeable differences in the activation phase (172, 174, 175). In addition, the GAP activity on transducin is enhanced by PDE $\gamma$  (109, 169, 176, 177) see PDE section). This provides an elegant mechanism for ensuring that excitation does not normally decay until  $G^*$  has bound to the effector, PDE. The same GAP complex is present in both rods and cones; however, its concentration is much higher in cones than in rods (178, 179). This has been suggested to contribute to the faster response kinetics of cones than rods.

Overexpression of PDE $\gamma$  in mouse rods can accelerate the shutoff of light response independent of the GAP complex, suggesting that the inhibitory sites on PDE  $\alpha$  and  $\beta$  are accessible to excess PDE $\gamma$  after endogenous PDE $\gamma$  has been displaced by  $G^*$  upon illumination (109). Overexpression also reduces the gain of transduction apparently through the "dominant negative effect" of interfering with the binding of  $G^*$  to endogenous PDE $\gamma$ .

Termination of phototransduction requires the shutoff of both  $R^*$  and  $G^*$ -PDE $^*$ , with the slower step determining the overall rate of response recovery. The identity of the rate-limiting step for rod recovery has been a long-standing question until recently (135, 180-183). By overexpressing the GAP complex in mouse rods, Krispel et al showed that the recovery of rod response was dramatically accelerated whereas overexpression of GRK1 had no effect (77). This experiment unequivocally demonstrated that the termination of  $G^*$ -PDE $^*$  is the rate-limiting step. It is worthwhile to note that the same step is not necessarily the rate-limiting step in cone recovery because there is a much higher concentration of the GAP complex in cones. The same "overexpression" technique can be used in cones to answer this question.

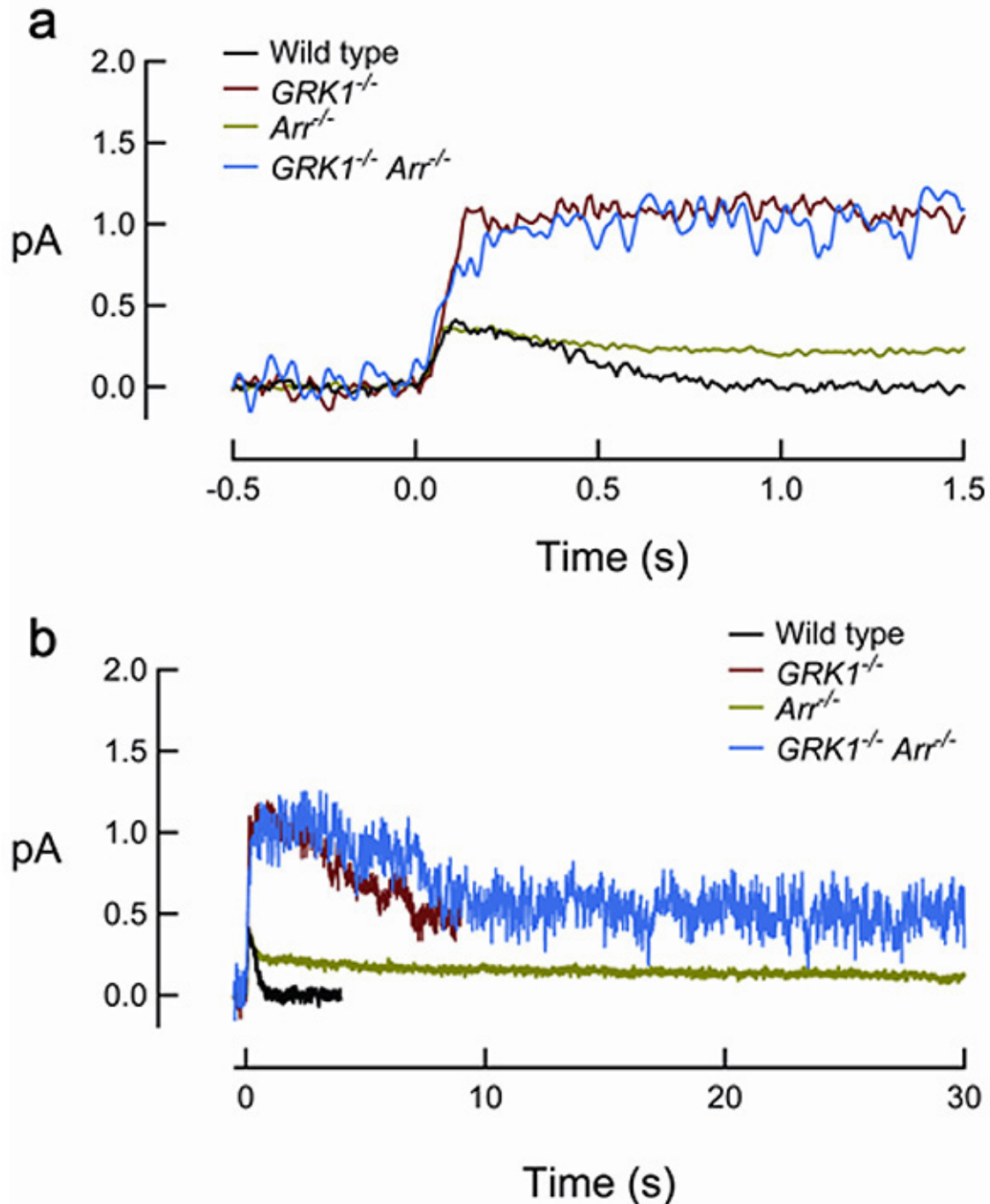


Figure 13. Form of the single-photon response from knockout mouse rods with deficient  $R^*$  termination on fast (a) and slow (b) time scales. Flashes were delivered at  $t = 0$ . Courtesy of Marie E. Burns.

Another implication of the above finding has to do with the question of the reproducibility of the single-photon response (see  $R^*$  Termination). Because  $G^*$  deactivation is 2.5 times slower than  $R^*$  deactivation (77), the slower  $G^*$  termination dictates the recovery kinetics of the single-photon response of rods. In addition to the multi-step involved in the shutoff of  $R^*$ , the activation of  $\sim 20$  transducin by one  $R^*$  can provide the necessary averaging for an otherwise stochastic process.

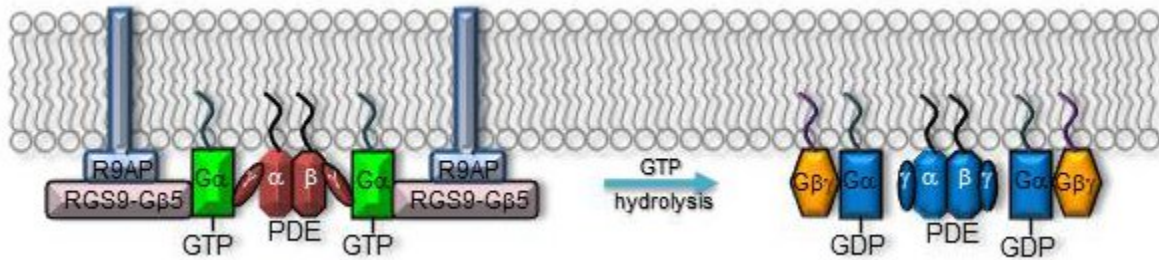


Figure 14. Schematic on the termination  $G^*-PDE^*$ .  $G\alpha^*-GTP$  binds to  $PDE\gamma$  and activates PDE. The deactivation of  $G\alpha^*-GTP$  is accelerated by the GAP complex, R9AP-RGS9-1-G $\beta$ 5L, in which RGS9-1 facilitates the hydrolysis of the bound GTP to GDP, leading to the re-formation of the inactive heterotrimeric  $G\alpha-GDP-G\beta\gamma$  and inactive PDE. This step was found to be the rate-limiting step of rod recovery (77).

## 16. Restoration of cGMP

The free concentration of cGMP is determined by the PDE-mediated hydrolysis and guanylate-cyclase (GC)-mediated synthesis. For the photoreceptor to recover, not only is the light-stimulated cGMP hydrolysis by PDE required to terminate as discussed in the previous sections, but the dark level of cGMP also has to be restored. There are two GCs in mouse photoreceptors: GC1 (GC-E) and GC2 (GC-F). GC1 is present in both rods and cones (184, 185), and GC2 is present only in rods (186). It seems that the basal activity of either GC1 or GC2 is sufficient to maintain dark current in rods (187, 188). Deletion of either GC has no significant impact on rod sensitivity. GC1 is important for cone function because cones degenerate in its absence. Deletion of both GC1 and GC2 rendered rod and cone photoreceptors nonfunctional and unstable (187).

GC activity is regulated by  $Ca^{2+}$ , mediated by the guanylate-cyclase-activating proteins (GCAPs). This regulation is the most important negative-feedback mechanism triggered by  $Ca^{2+}$  in the light. For topics on other  $Ca^{2+}$ -feedback effects and light adaptation, readers can refer to the following publications (101, 115, 189, 190).

GCAPs belong to a large family of calmodulin-like  $Ca^{2+}$ -binding proteins. Two GCAPs are present in mouse retinas, GCAP1 and GCAP2. Both GCAPs are expressed in mouse rods, but GCAP1 is primarily expressed in cones (191, 192). In darkness, the relatively high  $Ca^{2+}$  concentration promotes the formation of the  $Ca^{2+}$ -bound form of GCAPs, which inhibits GCs. When the  $Ca^{2+}$  concentration declines during the light response, the dissociation of  $Ca^{2+}$  allows GCAP to activate GC, thereby quickly restoring the basal cGMP concentration (Figure 15).

The two GCAP genes were knocked out in mouse simultaneously by taking advantage of their tail-to-tail arrangement on chromosome 17 (193). The flash response of  $GCAPs^{-/-}$  rods showed a larger amplitude and delayed decline compared to wild type, consistent with a delay in cGMP synthesis during recovery when the associated  $Ca^{2+}$ -feedback was removed. The power of  $Ca^{2+}$ -mediated regulation through GCAP can be appreciated from the fact that the single-photon response of  $GCAPs^{-/-}$  rods is nearly 5 times that of wild type, versus the 2-fold increase when pigment phosphorylation is prevented. By comparing the light response of  $GCAPs^{-/-}$  rods with that of wild-type rods, Burns et al. found that the activation of GC resulting from a change in  $Ca^{2+}$ -dependent GCAP activity occurs within  $\sim 40$  ms after the flash and in a highly cooperative manner, with a Hill coefficient of 4 (189). Therefore, the effect occurs much earlier than pigment phosphorylation, which is 80-100 msec after the flash (see  $R^*$  termination). The rapid feedback to GC has dual effects on photoreceptors, decreasing the dark-adapted flash sensitivity (132) and speeding the restoration of the dark current (36).



What are the functional differences between the two GCAPs? In vitro, GCAP1 activates GC1 more efficiently than GC2 (194, 195), whereas GCAP2 activates both GC1 and GC2 with similar efficiency (186, 196, 197). In vivo, transgenic GCAP1 can rescue the GCAPs<sup>-/-</sup> phenotype in rods and cones, as tested by single rod cell recordings and electroretinography, even in the absence of GCAP2 (198, 199). Expression of bovine GCAP2 in GCAPs<sup>-/-</sup> rods restored the recovery of rods to saturating flashes but failed to restore the recovery kinetics of responses initiated by sub-saturating flashes and, in particular, failed to rescue the fast initial phase of recovery (193), suggesting that GCAP1 is responsible for the initial rapid phase of response recovery. GCAP2 speeds up the recovery of flash responses and adjusts the operating range of rods to higher intensities of ambient illumination (200).

## 17. Mouse model of cone phototransduction

Recently, there have been substantial advances in the understanding of cone transduction with fish as the model (142, 143, 147, 201, 202). On the other hand, despite the enormous success in studying rod phototransduction by a combination of mouse genetics and suction-electrode recording in recent years, the usage of mouse as a model system for studying cone phototransduction has until recently been limited to ERG studies. This is mainly due to the rarity of cones (~3%) and the fragility of the cone outer segment (COS).

This hurdle was finally overcome by Pugh and colleagues (146, 203). The conventional suction-pipette recording, which involves drawing the ROS into the suction pipette ("OS in"), is not tolerated well by the more fragile COS. Instead, Pugh and colleagues drew a portion of the inner segment ("OS out") of a cone photoreceptor in a retinal slice into the suction pipette, allowing long, stable recordings. Previously, it was shown that the same information could be obtained by recording from either outer or inner segment of amphibian rods and cones (204) as expected from the nature of the circulating current.

To overcome the difficulty of identifying the ~3% cones in mouse retina, Pugh and colleagues used three different mouse lines. The first lacks the neural leucine zipper transcription factor (Nrl) (205), which drastically alters the cell fate of rod photoreceptors by turning them into cone-like photoreceptors (146, 206). The second expresses EGFP in mouse cones, which facilitates/verifies their identification (207). The third lacks the rod transducin  $\alpha$ -subunit (gnat1<sup>-/-</sup>), which blocks rod phototransduction (85).

In the case of the EGFP mouse line, background light is required in order to suppress the rod response so that the cone response can be isolated. As a result, the cone response is slightly light-adapted, therefore slightly faster and smaller for a given test-flash intensity than that from gnat1<sup>-/-</sup> or Nrl<sup>-/-</sup> cones. When this factor is taken into consideration, the light response properties of mouse cones recorded from the three mouse lines are very similar and are as expected from mammalian cones (Figure 16, Table 3) (203). Prominent among these features is that mouse cones are far more tolerant than mouse rods to bleached pigment. The dark current recovers substantially in both S- and M-type cones following strong flashes that bleach a substantial fraction of the pigment. One surprising finding, however, is that the inactivation of M pigment is more retarded than that of S pigment in the absence of GRK1, suggesting the existence of a GRK1-independent inactivation mechanism for the S pigment. Nrl<sup>-/-</sup> cones differ from wild type in certain respects. Their outer segments are shorter, more disordered and undergo a slow degeneration (206). In addition, in contrast to wild type, Nrl<sup>-/-</sup> cones express a much higher percentage of S-opsin. Thus, transgenic mice expressing EGFP in their cones and gnat1<sup>-/-</sup> mice are better than Nrl<sup>-/-</sup> mice for studying cone physiology.

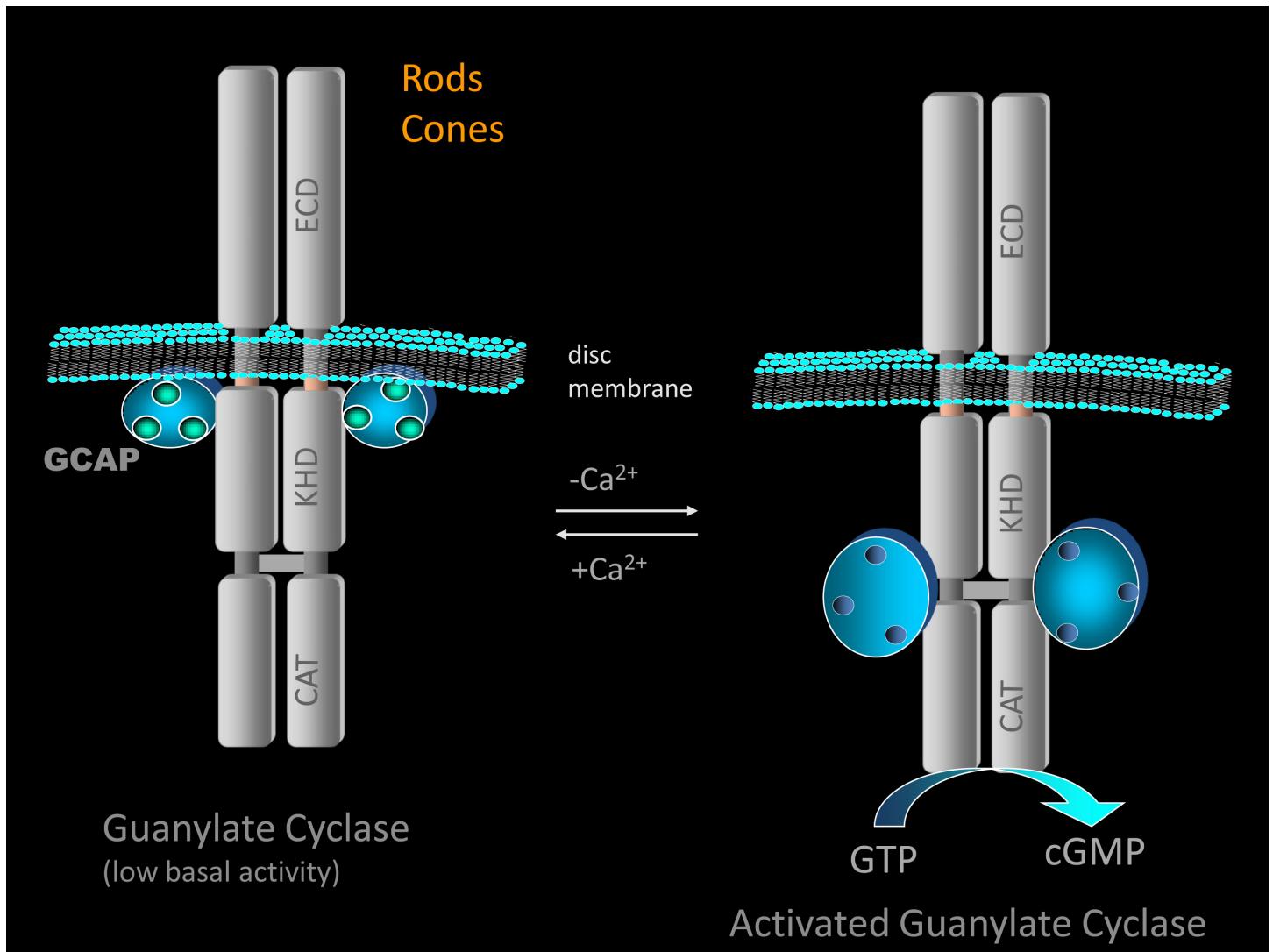


Figure 15. GCs and GCAPs in rods and cones. ECD, extracellular domain, KHD, kinase homology domain, CAT, catalytic domain. Courtesy of Wolfgang Baehr.

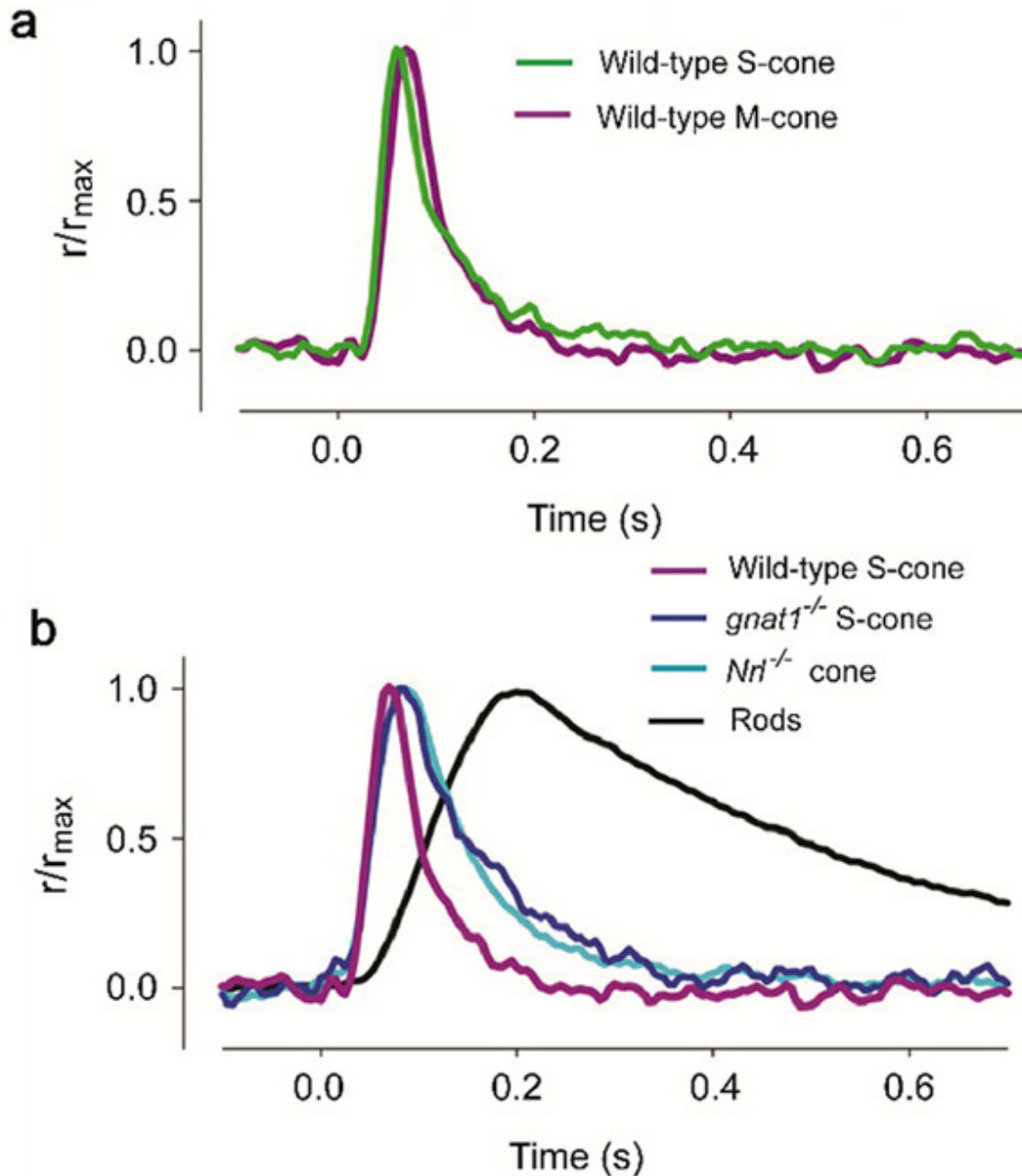


Figure 16. Flash responses of mouse cone photoreceptors from different genotypes. a. Comparison of the average response of S-cones to 361-nm flashes and M-cones to 510-nm flashes. b. Comparison of the average flash responses to 361-nm flashes of wild-type S-cones,  $gnat1^{-/-}$  S-cones,  $Nrl^{-/-}$  cones, and rods recorded under the same "OS out" conditions. Each trace is scaled to unity at its peak. Data from Fig. 4E & F of Nikonov et al., 2006 (203) with permission from the Rockefeller University Press.

Table 3. Kinetic and Sensitivity Parameters of mouse rods and cones.  $I_d$ , dark current.  $t_p$ , the time to peak of the dim-flash response.  $\tau_D$ , the dominant recovery time constant.  $I_{1/2}$ , Flash strength that elicited a half-maximal response, uncorrected for pigment bleaching for cones. Data from Table 1 of Nikonov, 2006 (203)

	$I_d$ (pA)	$t_p$ (ms)	$\tau_D$ (ms)	$I_{1/2}$ (photons $\mu\text{m}^{-2} \text{s}^{-1}$ )
S-cone (n = 21)	$6 \pm 1$	$73 \pm 5$	$73 \pm 10$	$(1.8 \pm 0.6) \times 10^5$
M-cone (n = 8)	$8 \pm 2$	$63 \pm 5$	$68 \pm 18$	$(2.5 \pm 0.9) \times 10^5$
Rods (n = 26)	$20 \pm 6$	$205 \pm 10$	$235 \pm 20$	350

## 18. Concluding remarks

In the past decade, great progress has been made in using mouse models to elucidate the mechanisms of activation and termination of the rod phototransduction pathway. Although there are still questions to be answered about the rod pathway such as the reproducibility of the single-photon response, the current frontier of phototransduction research lies in cones, which, for human vision, are far more important than rods. The recent success in recording from single mouse cones ushers in a new era in research on vertebrate cone phototransduction. Many long standing questions, e.g., the mechanisms for the enormous ability of cones to adapt to light, and the differences between rods and cones in sensitivity and kinetics, can now be addressed with a combination of mouse genetics and electrophysiology.

## About the Author



Dr. Yingbin Fu is presently an Assistant Professor in the Department of Ophthalmology and Visual Science, John Moran Eye Center, University of Utah. He received his B.S in Biochemistry at Peking University, Beijing, China. After receiving his Ph.D. in Biochemistry at Michigan State University, East Lansing, Michigan, Dr. Fu's interests turned into retina and he joined Dr. King-Wai Yau's lab as a postdoc fellow at the Johns Hopkins University School of Medicine in Baltimore, Maryland. His postdoc experience turned out to be quite fruitful after he successfully brought his expertise in *Xenopus* and mouse genetics to the Yau lab, a world-class electrophysiology lab. Dr. Fu made significant discoveries on the role of visual pigments in rod and cone phototransduction, and the role of melanopsin in intrinsically photosensitive retinal ganglion cells. After moving to Utah to establish his own lab, Dr. Fu's research primarily focuses on two objectives: 1. To understand the mechanisms governing the assembly/trafficking of key photoreceptor proteins and its role in photoreceptor survival; 2. To perform functional characterization on genetic variants that are associated with age-related macular degeneration (AMD) with animal models. Email: [yingbin.fu@hsc.utah.edu](mailto:yingbin.fu@hsc.utah.edu)

## References

1. Baylor D.A., Lamb T.D., Yau K.W. *The membrane current of single rod outer segments.* . J Physiol. 1979;288:589–611. PubMed PMID: 112242.
2. Carter-Dawson L.D., LaVail M.M. *Rods and cones in the mouse retina. I. Structural analysis using light and electron microscopy.* . J Comp Neurol. 1979;188(2):245–62. PubMed PMID: 500858.
3. Humphries M.M. et al. *Retinopathy induced in mice by targeted disruption of the rhodopsin gene.* . Nat Genet. 1997;15(2):216–9. PubMed PMID: 9020854.
4. Lem J. et al. *Morphological, physiological, and biochemical changes in rhodopsin knockout mice.* . Proc Natl Acad Sci U S A. 1999;96(2):736–41. PubMed PMID: 9892703.
5. Harosi F.I. *Absorption spectra and linear dichroism of some amphibian photoreceptors.* . J Gen Physiol. 1975;66(3):357–82. PubMed PMID: 808586.
6. Hagins W.A., Penn R.D., Yoshikami S. *Dark current and photocurrent in retinal rods.* . Biophys J. 1970;10(5):380–412. PubMed PMID: 5439318.
7. Hecht S., Shlaer S., Pirenne M.H. *Energy, Quanta, and Vision.* . J Gen Physiol. 1942;25(6):819–840. PubMed PMID: 19873316.
8. Young R.W. *The renewal of photoreceptor cell outer segments.* . J Cell Biol. 1967;33(1):61–72. PubMed PMID: 6033942.
9. Young R.W., Droz B. *The renewal of protein in retinal rods and cones.* . J Cell Biol. 1968;39(1):169–84. PubMed PMID: 5692679.
10. Young R.W., Bok D. *Participation of the retinal pigment epithelium in the rod outer segment renewal process.* . J Cell Biol. 1969;42(2):392–403. PubMed PMID: 5792328.
11. LaVail M.M. *Kinetics of rod outer segment renewal in the developing mouse retina.* . J Cell Biol. 1973;58(3):650–61. PubMed PMID: 4747920.
12. Caravaggio L.L., Bonting S.L. *The rhodopsin cycle in the developing vertebrate retina. II. Correlative study in normal mice and in mice with hereditary retinal degeneration.* . Exp Eye Res. 1963;2:12–9. PubMed PMID: 14018516.
13. Luo D.G., Yau K.W. *Rod sensitivity of neonatal mouse and rat.* . J Gen Physiol. 2005;126(3):263–9. PubMed PMID: 16129773.
14. Ratto G.M. et al. *Development of the light response in neonatal mammalian rods.* . Nature. 1991;351(6328):654–7. PubMed PMID: 2052091.
15. Baylor D.A., Lamb T.D., Yau K.W. *Responses of retinal rods to single photons.* . J Physiol. 1979;288:613–34. PubMed PMID: 112243.
16. Arshavsky V.Y., Lamb T.D., Pugh E.N. Jr. *G proteins and phototransduction.* . Annu Rev Physiol. 2002;64:153–87. PubMed PMID: 11826267.
17. Lamb T.D. *Gain and kinetics of activation in the G-protein cascade of phototransduction.* . Proc Natl Acad Sci U S A. 1996;93(2):566–70. PubMed PMID: 8570596.
18. Lamb T.D., Pugh E.N. Jr. *A quantitative account of the activation steps involved in phototransduction in amphibian photoreceptors.* . J Physiol. 1992;449:719–58. PubMed PMID: 1326052.
19. Pugh E.N. Jr, Lamb T.D. *Amplification and kinetics of the activation steps in phototransduction.* . Biochim Biophys Acta. 1993;1141(2-3):111–49. PubMed PMID: 8382952.
20. Applebury M.L. et al. *The murine cone photoreceptor: a single cone type expresses both S and M opsins with retinal spatial patterning.* . Neuron. 2000;27(3):513–23. PubMed PMID: 11055434.
21. Palczewski K. et al. *Crystal structure of rhodopsin: A G protein-coupled receptor.* . Science. 2000;289(5480):739–45. PubMed PMID: 10926528.
22. Stenkamp R.E., Teller D.C., Palczewski K. *Crystal structure of rhodopsin: a G-protein-coupled receptor.* . Chembiochem. 2002;3(10):963–7. PubMed PMID: 12362360.

23. Bridges, C.D.B., *The rhodopsin-porphyrpsin visual system*. Handbook of Sensory Physiology, VII/1. Photochemistry of Vision, ed. H.J.A. Dartnall. Vol. VII/1. 1972, Berlin-Heidelberg-NewYork: Springer. 417-480.
24. Dartnall H.J., Lythgoe J.N. *The spectral clustering of visual pigments*. . Vision Res. 1965;5(3):81–100. PubMed PMID: 5862952.
25. Wald G. *On the Distribution of Vitamins a(1) and a(2)*. . J Gen Physiol. 1939;22(3):391–415. PubMed PMID: 19873110.
26. Wald G. *Vitamin a in Eye Tissues*. . J Gen Physiol. 1935;18(6):905–915. PubMed PMID: 19872899.
27. Redmond T.M.et al. *Rpe65 is necessary for production of 11-cis-vitamin A in the retinal visual cycle*. . Nat Genet. 1998;20(4):344–51. PubMed PMID: 9843205.
28. Woodruff M.L.et al. *Spontaneous activity of opsin apoprotein is a cause of Leber congenital amaurosis*. . Nat Genet. 2003;35(2):158–64. PubMed PMID: 14517541.
29. Li T.et al. *Constitutive activation of phototransduction by K296E opsin is not a cause of photoreceptor degeneration*. . Proc Natl Acad Sci U S A. 1995;92(8):3551–5. PubMed PMID: 7724596.
30. Baylor D.A., Matthews G., Yau K.W. *Two components of electrical dark noise in toad retinal rod outer segments*. . J Physiol. 1980;309:591–621. PubMed PMID: 6788941.
31. Aho A.C.et al. *Low retinal noise in animals with low body temperature allows high visual sensitivity*. . Nature. 1988;334(6180):348–50. PubMed PMID: 3134619.
32. Autrum H. *Über kleinste Reize bei Sinnesorganen*. . Biologisches Zentralblatt. 1943;63:209–236.
33. Barlow H.B. *Retinal noise and absolute threshold*. . J Opt Soc Am. 1956;46(8):634–9. PubMed PMID: 13346424.
34. Donner K. *Noise and the absolute thresholds of cone and rod vision*. . Vision Res. 1992;32(5):853–66. PubMed PMID: 1604854.
35. Yau K.W., Matthews G., Baylor D.A. *Thermal activation of the visual transduction mechanism in retinal rods*. . Nature. 1979;279(5716):806–7. PubMed PMID: 109776.
36. Burns M.E.et al. *Dynamics of cyclic GMP synthesis in retinal rods*. . Neuron. 2002;36(1):81–91. PubMed PMID: 12367508.
37. Barlow H.B. *Increment thresholds at low intensities considered as signal/noise discriminations*. . J Physiol. 1957;136(3):469–88. PubMed PMID: 13429514.
38. Kefalov V.et al. *Role of visual pigment properties in rod and cone phototransduction*. . Nature. 2003;425(6957):526–31. PubMed PMID: 14523449.
39. Rieke F., Baylor D.A. *Origin and functional impact of dark noise in retinal cones*. . Neuron. 2000;26(1):181–6. PubMed PMID: 10798402.
40. Fu Y.et al. *Quantal noise from human red cone pigment*. . Nat Neurosci. 2008;11(5):565–71. PubMed PMID: 18425122.
41. Schnapf J.L.et al. *Visual transduction in cones of the monkey Macaca fascicularis*. . J Physiol. 1990;427:681–713. PubMed PMID: 2100987.
42. Schneeweis D.M., Schnapf J.L. *The photovoltage of macaque cone photoreceptors: adaptation, noise, and kinetics*. . J Neurosci. 1999;19(4):1203–16. PubMed PMID: 9952398.
43. Holcman D., Korenbrot J.I. *The limit of photoreceptor sensitivity: molecular mechanisms of dark noise in retinal cones*. . J Gen Physiol. 2005;125(6):641–60. PubMed PMID: 15928405.
44. Bridges C.D. *Spectroscopic properties of porphyropsins*. . Vision Res. 1967;7(5):349–69. PubMed PMID: 5613301.
45. Donner K., Firsov M.L., Govardovskii V.I. *The frequency of isomerization-like 'dark' events in rhodopsin and porphyropsin rods of the bull-frog retina*. . J Physiol. 1990;428:673–92. PubMed PMID: 2231428.
46. Ala-Laurila P.et al. *Chromophore switch from 11-cis-dehydroretinal (A2) to 11-cis-retinal (A1) decreases dark noise in salamander red rods*. . J Physiol. 2007;585(Pt 1):57–74. PubMed PMID: 17884920.
47. Kefalov V.J.et al. *Breaking the Covalent Bond- A Pigment Property that Contributes to Desensitization in Cones*. . Neuron. 2005;46(6):879–90. PubMed PMID: 15953417.

48. Miller J.L., Picones A., Korenbrot J.I. *Differences in transduction between rod and cone photoreceptors: an exploration of the role of calcium homeostasis.* . Curr Opin Neurobiol. 1994;4(4):488–95. PubMed PMID: 7812136.
49. Nakatani K., Yau K.W. *Sodium-dependent calcium extrusion and sensitivity regulation in retinal cones of the salamander.* . J Physiol. 1989;409:525–48. PubMed PMID: 2479741.
50. Tachibanaki S. et al. *Molecular mechanisms characterizing cone photoresponses.* . Photochem Photobiol. 2007;83(1):19–26. PubMed PMID: 16706600.
51. Ma J. et al. *A visual pigment expressed in both rod and cone photoreceptors.* . Neuron. 2001;32(3):451–61. PubMed PMID: 11709156.
52. Perry R.J., McNaughton P.A. *Response properties of cones from the retina of the tiger salamander.* . J Physiol. 1991;433:561–87. PubMed PMID: 1841958.
53. Hubbard R., Wald G. *Cis-trans isomers of vitamin A and retinene in the rhodopsin system.* . J Gen Physiol. 1952;36(2):269–315. PubMed PMID: 13011282.
54. Wald G. *The chemistry of rod vision.* . Science. 1951;113(2933):287–91. PubMed PMID: 14817272.
55. Lythgoe R.J., Quilliam J.P. *The relation of transient orange to visual purple and indicator yellow.* . J Physiol. 1938;94(3):399–410. PubMed PMID: 16995053.
56. Wald G. *On Rhodopsin in Solution.* . J Gen Physiol. 1938;21(6):795–832. PubMed PMID: 19873085.
57. Wald G., Durell J., St George C.C. *The light reaction in the bleaching of rhodopsin.* . Science. 1950;111(2877):179–81. PubMed PMID: 15403120.
58. Hubbard R., Kropf A. *The Action of Light on Rhodopsin.* . Proc Natl Acad Sci U S A. 1958;44(2):130–9. PubMed PMID: 16590155.
59. Okada T., Palczewski K. *Crystal structure of rhodopsin: implications for vision and beyond.* . Curr Opin Struct Biol. 2001;11(4):420–6. PubMed PMID: 11495733.
60. Imai H. et al. *Photochemical and biochemical properties of chicken blue-sensitive cone visual pigment.* . Biochemistry. 1997;36(42):12773–9. PubMed PMID: 9335534.
61. Kuwayama S. et al. *Amino acid residues responsible for the meta-III decay rates in rod and cone visual pigments.* . Biochemistry. 2005;44(6):2208–15. PubMed PMID: 15697246.
62. Shichida Y. et al. *Is chicken green-sensitive cone visual pigment a rhodopsin-like pigment? A comparative study of the molecular properties between chicken green and rhodopsin.* . Biochemistry. 1994;33(31):9040–4. PubMed PMID: 8049204.
63. Vought B.W. et al. *Photochemistry of the primary event in short-wavelength visual opsins at low temperature.* . Biochemistry. 1999;38(35):11287–97. PubMed PMID: 10471278.
64. Nathans J. *Determinants of visual pigment absorbance: identification of the retinylidene Schiff's base counterion in bovine rhodopsin.* . Biochemistry. 1990;29(41):9746–52. PubMed PMID: 1980212.
65. Sakmar T.P., Franke R.R., Khorana H.G. *Glutamic acid-113 serves as the retinylidene Schiff base counterion in bovine rhodopsin.* . Proc Natl Acad Sci U S A. 1989;86(21):8309–13. PubMed PMID: 2573063.
66. Zhukovsky E.A., Oprian D.D. *Effect of carboxylic acid side chains on the absorption maximum of visual pigments.* . Science. 1989;246(4932):928–30. PubMed PMID: 2573154.
67. Yan E.C. et al. *Retinal counterion switch in the photoactivation of the G protein-coupled receptor rhodopsin.* . Proc Natl Acad Sci U S A. 2003;100(16):9262–7. PubMed PMID: 12835420.
68. Dukkupati A. et al. *Phototransduction by vertebrate ultraviolet visual pigments: protonation of the retinylidene Schiff base following photobleaching.* . Biochemistry. 2002;41(31):9842–51. PubMed PMID: 12146950.
69. Kusnetzow A.K. et al. *Vertebrate ultraviolet visual pigments: protonation of the retinylidene Schiff base and a counterion switch during photoactivation.* . Proc Natl Acad Sci U S A. 2004;101(4):941–6. PubMed PMID: 14732701.
70. McBee J.K. et al. *Confronting complexity: the interlink of phototransduction and retinoid metabolism in the vertebrate retina.* . Prog Retin Eye Res. 2001;20(4):469–529. PubMed PMID: 11390257.
71. Calvert P.D. et al. *Membrane protein diffusion sets the speed of rod phototransduction.* . Nature. 2001;411(6833):90–4. PubMed PMID: 11333983.

72. Liang, Y., et al., *Rhodopsin signaling and organization in heterozygote rhodopsin knockout mice*. J Biol Chem, 2004
73. Kropf A. *Photosensitivity and quantum efficiency of photoisomerization in rhodopsin and retinal*. . Methods Enzymol. 1982;81:384–92. PubMed PMID: 7098885.
74. Leskov I.B.et al. *The gain of rod phototransduction: reconciliation of biochemical and electrophysiological measurements*. . Neuron. 2000;27(3):525–37. PubMed PMID: 11055435.
75. Heck M., Hofmann K.P. *Maximal rate and nucleotide dependence of rhodopsin-catalyzed transducin activation: initial rate analysis based on a double displacement mechanism*. . J Biol Chem. 2001;276(13):10000–9. PubMed PMID: 11116153.
76. Makino C.L., Wen X.H., Lem J. *Piecing together the timetable for visual transduction with transgenic animals*. . Curr Opin Neurobiol. 2003;13(4):404–12. PubMed PMID: 12965286.
77. Krispel C.M.et al. *RGS expression rate-limits recovery of rod photoresponses*. . Neuron. 2006;51(4):409–16. PubMed PMID: 16908407.
78. Fung B.K., Lieberman B.S., Lee R.H. *A third form of the G protein beta subunit. 2. Purification and biochemical properties*. . J Biol Chem. 1992;267(34):24782–8. PubMed PMID: 1332966.
79. Lee R.H.et al. *A third form of the G protein beta subunit. 1. Immunochemical identification and localization to cone photoreceptors*. . J Biol Chem. 1992;267(34):24776–81. PubMed PMID: 1447215.
80. Lerea C.L.et al. *Identification of specific transducin alpha subunits in retinal rod and cone photoreceptors*. . Science. 1986;234(4772):77–80. PubMed PMID: 3529395.
81. Peng Y.W.et al. *Retinal rods and cones have distinct G protein beta and gamma subunits*. . Proc Natl Acad Sci U S A. 1992;89(22):10882–6. PubMed PMID: 1438293.
82. Fukada Y.et al. *Phosphorylation of iodopsin, chicken red-sensitive cone visual pigment*. . Biochemistry. 1990;29(43):10102–6. PubMed PMID: 2271641.
83. Kokame K.et al. *Lipid modification at the N terminus of photoreceptor G-protein alpha-subunit*. . Nature. 1992;359(6397):749–52. PubMed PMID: 1436039.
84. Neubert T.A.et al. *The rod transducin alpha subunit amino terminus is heterogeneously fatty acylated*. . J Biol Chem. 1992;267(26):18274–7. PubMed PMID: 1326520.
85. Calvert P.D.et al. *Phototransduction in transgenic mice after targeted deletion of the rod transducin alpha-subunit*. . Proc Natl Acad Sci U S A. 2000;97(25):13913–8. PubMed PMID: 11095744.
86. Fu Y.et al. *Intrinsically photosensitive retinal ganglion cells detect light with a vitamin A-based photopigment, melanopsin*. . Proc Natl Acad Sci U S A. 2005;102(29):10339–44. PubMed PMID: 16014418.
87. Hattar S.et al. *Melanopsin and rod-cone photoreceptive systems account for all major accessory visual functions in mice*. . Nature. 2003;424(6944):76–81. PubMed PMID: 12808468.
88. Lyubarsky A.L.et al. *Functionally rodless mice: transgenic models for the investigation of cone function in retinal disease and therapy*. . Vision Res. 2002;42(4):401–15. PubMed PMID: 11853756.
89. Hao W.et al. *Evidence for two apoptotic pathways in light-induced retinal degeneration*. . Nat Genet. 2002;32(2):254–60. PubMed PMID: 12219089.
90. Kassai H.et al. *Farnesylation of retinal transducin underlies its translocation during light adaptation*. . Neuron. 2005;47(4):529–39. PubMed PMID: 16102536.
91. Sokolov M.et al. *Massive light-driven translocation of transducin between the two major compartments of rod cells: a novel mechanism of light adaptation*. . Neuron. 2002;34(1):95–106. PubMed PMID: 11931744.
92. Elias R.V.et al. *Temporal kinetics of the light/dark translocation and compartmentation of arrestin and alpha-transducin in mouse photoreceptor cells*. . Mol Vis. 2004;10:672–81. PubMed PMID: 15467522.
93. Coleman J.E., Semple-Rowland S.L. *GC1 deletion prevents light-dependent arrestin translocation in mouse cone photoreceptor cells*. . Invest Ophthalmol Vis Sci. 2005;46(1):12–6. PubMed PMID: 15623748.
94. Kennedy M.J., Dunn F.A., Hurley J.B. *Visual pigment phosphorylation but not transducin translocation can contribute to light adaptation in zebrafish cones*. . Neuron. 2004;41(6):915–28. PubMed PMID: 15046724.
95. Chen J.et al. *Light Threshold-Controlled Cone {alpha}-Transducin Translocation*. . Invest Ophthalmol Vis Sci. 2007;48(7):3350–5. PubMed PMID: 17591908.



96. Baehr W., Devlin M.J., Applebury M.L. *Isolation and characterization of cGMP phosphodiesterase from bovine rod outer segments.* . J Biol Chem. 1979;254(22):11669–77. PubMed PMID: 227876.
97. Deterre P.et al. *cGMP phosphodiesterase of retinal rods is regulated by two inhibitory subunits.* . Proc Natl Acad Sci U S A. 1988;85(8):2424–8. PubMed PMID: 2833739.
98. Hurley J.B., Stryer L. *Purification and characterization of the gamma regulatory subunit of the cyclic GMP phosphodiesterase from retinal rod outer segments.* . J Biol Chem. 1982;257(18):11094–9. PubMed PMID: 6286681.
99. Anant J.S.et al. *In vivo differential prenylation of retinal cyclic GMP phosphodiesterase catalytic subunits.* . J Biol Chem. 1992;267(2):687–90. PubMed PMID: 1309771.
100. Qin N., Baehr W. *Expression and mutagenesis of mouse rod photoreceptor cGMP phosphodiesterase.* . J Biol Chem. 1994;269(5):3265–71. PubMed PMID: 8106363.
101. Pugh, E.N., Jr. and T.D. Lamb, *Phototransduction in Vertebrate Rods and Cones: Molecular Mechanisms of Amplification, Recovery and Light Adaptation.*, in *Handbook of Biological Physics*, D.G. Stavenga, W.J. de Grip, and E.N. Pugh, Jr., Editors. 2000, Elsevier Science B.V.: Amsterdam. p. 183-255.
102. Tsang S.H.et al. *Retinal degeneration in mice lacking the gamma subunit of the rod cGMP phosphodiesterase.* . Science. 1996;272(5264):1026–9. PubMed PMID: 8638127.
103. Carter-Dawson L.D., LaVail M.M., Sidman R.L. *Differential effect of the rd mutation on rods and cones in the mouse retina.* . Invest Ophthalmol Vis Sci. 1978;17(6):489–98. PubMed PMID: 659071.
104. LaVail M.M., Sidman R.L. *C57BL-6J mice with inherited retinal degeneration.* . Arch Ophthalmol. 1974;91(5):394–400. PubMed PMID: 4595403.
105. Bowes C.et al. *Retinal degeneration in the rd mouse is caused by a defect in the beta subunit of rod cGMP-phosphodiesterase.* . Nature. 1990;347(6294):677–80. PubMed PMID: 1977087.
106. Pittler S.J., Baehr W. *Identification of a nonsense mutation in the rod photoreceptor cGMP phosphodiesterase beta-subunit gene of the rd mouse.* . Proc Natl Acad Sci U S A. 1991;88(19):8322–6. PubMed PMID: 1656438.
107. Freedman M.S.et al. *Regulation of mammalian circadian behavior by non-rod, non-cone, ocular photoreceptors.* . Science. 1999;284(5413):502–4. PubMed PMID: 10205061.
108. Lucas R.J.et al. *Regulation of the mammalian pineal by non-rod, non-cone, ocular photoreceptors.* . Science. 1999;284(5413):505–7. PubMed PMID: 10205062.
109. Tsang S.H.et al. *Role for the target enzyme in deactivation of photoreceptor G protein in vivo.* . Science. 1998;282(5386):117–21. PubMed PMID: 9756475.
110. Luo D.G., Xue T., Yau K.W. *How vision begins: an odyssey.* . Proc Natl Acad Sci U S A. 2008;105(29):9855–62. PubMed PMID: 18632568.
111. Fesenko E.E., Kolesnikov S.S., Lyubarsky A.L. *Induction by cyclic GMP of cationic conductance in plasma membrane of retinal rod outer segment.* . Nature. 1985;313(6000):310–3. PubMed PMID: 2578616.
112. Yau K.W., Nakatani K. *Light-suppressible, cyclic GMP-sensitive conductance in the plasma membrane of a truncated rod outer segment.* . Nature. 1985;317(6034):252–5. PubMed PMID: 2995816.
113. Kaupp U.B., Seifert R. *Cyclic nucleotide-gated ion channels.* . Physiol Rev. 2002;82(3):769–824. PubMed PMID: 12087135.
114. Molday, R.S. and U.B. Kaupp, *Ion channels of vertebrate photoreceptors*, in *Handbook of Biological Physics*, D.G. Stavenga, W.J. de Grip, and E.N. Pugh, Jr., Editors. 2000, Elsevier Science B.V.: Amsterdam.
115. Yau K.W. *Phototransduction mechanism in retinal rods and cones. The Friedenwald Lecture.* . Invest Ophthalmol Vis Sci. 1994;35(1):9–32. PubMed PMID: 7507907.
116. Karpen J.W.et al. *Gating kinetics of the cyclic-GMP-activated channel of retinal rods: flash photolysis and voltage-jump studies.* . Proc Natl Acad Sci U S A. 1988;85(4):1287–91. PubMed PMID: 2448798.
117. Weitz D.et al. *Subunit stoichiometry of the CNG channel of rod photoreceptors.* . Neuron. 2002;36(5):881–9. PubMed PMID: 12467591.
118. Zheng J., Trudeau M.C., Zagotta W.N. *Rod cyclic nucleotide-gated channels have a stoichiometry of three CNGB1 subunits and one CNGA1 subunit.* . Neuron. 2002;36(5):891–6. PubMed PMID: 12467592.

119. Zhong H.et al. *The heteromeric cyclic nucleotide-gated channel adopts a 3A:1B stoichiometry.* . Nature. 2002;420(6912):193–8. PubMed PMID: 12432397.
120. Peng C., Rich E.D., Varnum M.D. *Subunit configuration of heteromeric cone cyclic nucleotide-gated channels.* . Neuron. 2004;42(3):401–10. PubMed PMID: 15134637.
121. Biel M.et al. *Selective loss of cone function in mice lacking the cyclic nucleotide-gated channel CNG3.* . Proc Natl Acad Sci U S A. 1999;96(13):7553–7. PubMed PMID: 10377453.
122. Finn J.T., Grunwald M.E., Yau K.W. *Cyclic nucleotide-gated ion channels: an extended family with diverse functions.* . Annu Rev Physiol. 1996;58:395–426. PubMed PMID: 8815801.
123. Matulef K., Zagotta W.N. *Cyclic nucleotide-gated ion channels.* . Annu Rev Cell Dev Biol. 2003;19:23–44. PubMed PMID: 14570562.
124. Dryja T.P.et al. *Mutations in the gene encoding the alpha subunit of the rod cGMP-gated channel in autosomal recessive retinitis pigmentosa.* . Proc Natl Acad Sci U S A. 1995;92(22):10177–81. PubMed PMID: 7479749.
125. Kohl S.et al. *Total colourblindness is caused by mutations in the gene encoding the alpha-subunit of the cone photoreceptor cGMP-gated cation channel.* . Nat Genet. 1998;19(3):257–9. PubMed PMID: 9662398.
126. Kohl S.et al. *Mutations in the CNGB3 gene encoding the beta-subunit of the cone photoreceptor cGMP-gated channel are responsible for achromatopsia (ACHM3) linked to chromosome 8q21.* . Hum Mol Genet. 2000;9(14):2107–16. PubMed PMID: 10958649.
127. Huttl S.et al. *Impaired channel targeting and retinal degeneration in mice lacking the cyclic nucleotide-gated channel subunit CNGB1.* . J Neurosci. 2005;25(1):130–8. PubMed PMID: 15634774.
128. Chen C., Nakatani K., Koutalos Y. *Free magnesium concentration in salamander photoreceptor outer segments.* . J Physiol. 2003;553(Pt 1):125–35. PubMed PMID: 14500766.
129. Kuhn H., Wilden U. *Deactivation of photoactivated rhodopsin by rhodopsin-kinase and arrestin.* . J Recept Res. 1987;7(1-4):283–98. PubMed PMID: 3040978.
130. Wilden U., Hall S.W., Kuhn H. *Phosphodiesterase activation by photoexcited rhodopsin is quenched when rhodopsin is phosphorylated and binds the intrinsic 48-kDa protein of rod outer segments.* . Proc Natl Acad Sci U S A. 1986;83(5):1174–8. PubMed PMID: 3006038.
131. Ohguro H.et al. *Rhodopsin phosphorylation and dephosphorylation in vivo.* . J Biol Chem. 1995;270(24):14259–62. PubMed PMID: 7782279.
132. Mendez A.et al. *Rapid and reproducible deactivation of rhodopsin requires multiple phosphorylation sites.* . Neuron. 2000;28(1):153–64. PubMed PMID: 11086991.
133. Gibson S.K., Parkes J.H., Liebman P.A. *Phosphorylation modulates the affinity of light-activated rhodopsin for G protein and arrestin.* . Biochemistry. 2000;39(19):5738–49. PubMed PMID: 10801324.
134. Hamer R.D.et al. *Multiple steps of phosphorylation of activated rhodopsin can account for the reproducibility of vertebrate rod single-photon responses.* . J Gen Physiol. 2003;122(4):419–44. PubMed PMID: 12975449.
135. Rieke F., Baylor D.A. *Origin of reproducibility in the responses of retinal rods to single photons.* . Biophys J. 1998;75(4):1836–57. PubMed PMID: 9746525.
136. Whitlock G.G., Lamb T.D. *Variability in the time course of single photon responses from toad rods: termination of rhodopsin's activity.* . Neuron. 1999;23(2):337–51. PubMed PMID: 10399939.
137. Doan T.et al. *Multiple phosphorylation sites confer reproducibility of the rod's single-photon responses.* . Science. 2006;313(5786):530–3. PubMed PMID: 16873665.
138. Chen J.et al. *Mechanisms of rhodopsin inactivation in vivo as revealed by a COOH-terminal truncation mutant.* . Science. 1995;267(5196):374–7. PubMed PMID: 7824934.
139. Chen C.K.et al. *Abnormal photoresponses and light-induced apoptosis in rods lacking rhodopsin kinase.* . Proc Natl Acad Sci U S A. 1999;96(7):3718–22. PubMed PMID: 10097103.
140. Kuwayama S.et al. *Conserved proline residue at position 189 in cone visual pigments as a determinant of molecular properties different from rhodopsins.* . Biochemistry. 2002;41(51):15245–52. PubMed PMID: 12484762.
141. Rinner O.et al. *Knockdown of cone-specific kinase GRK7 in larval zebrafish leads to impaired cone response recovery and delayed dark adaptation.* . Neuron. 2005;47(2):231–42. PubMed PMID: 16039565.

142. Tachibanaki S. et al. *Highly effective phosphorylation by G protein-coupled receptor kinase 7 of light-activated visual pigment in cones.* . Proc Natl Acad Sci U S A. 2005;102(26):9329–34. PubMed PMID: 15958532.
143. Tachibanaki S., Tsushima S., Kawamura S. *Low amplification and fast visual pigment phosphorylation as mechanisms characterizing cone photoresponses.* . Proc Natl Acad Sci U S A. 2001;98(24):14044–9. PubMed PMID: 11707584.
144. Weiss E.R. et al. *Species-specific differences in expression of G-protein-coupled receptor kinase (GRK) 7 and GRK1 in mammalian cone photoreceptor cells: implications for cone cell phototransduction.* . J Neurosci. 2001;21(23):9175–84. PubMed PMID: 11717351.
145. Lyubarsky A.L. et al. *Mice lacking G-protein receptor kinase 1 have profoundly slowed recovery of cone-driven retinal responses.* . J Neurosci. 2000;20(6):2209–17. PubMed PMID: 10704496.
146. Nikonov S.S. et al. *Photoreceptors of Nrl -/- mice coexpress functional S- and M-cone opsins having distinct inactivation mechanisms.* . J Gen Physiol. 2005;125(3):287–304. PubMed PMID: 15738050.
147. Wada Y. et al. *GRK1 and GRK7: unique cellular distribution and widely different activities of opsin phosphorylation in the zebrafish rods and cones.* . J Neurochem. 2006;98(3):824–37. PubMed PMID: 16787417.
148. Tachibanaki, S., et al., *Molecular Mechanisms Characterizing Cone Photoresponses.* Photochem Photobiol, 2006
149. Chen C.K. et al. *Ca(2+)-dependent interaction of recoverin with rhodopsin kinase.* . J Biol Chem. 1995;270(30):18060–6. PubMed PMID: 7629115.
150. Kawamura S. *Light-sensitivity modulating protein in frog rods.* . Photochem Photobiol. 1992;56(6):1173–80. PubMed PMID: 1337215.
151. Kawamura S. *Rhodopsin phosphorylation as a mechanism of cyclic GMP phosphodiesterase regulation by S-modulin.* . Nature. 1993;362(6423):855–7. PubMed PMID: 8386803.
152. Klenchin V.A., Calvert P.D., Bownds M.D. *Inhibition of rhodopsin kinase by recoverin. Further evidence for a negative feedback system in phototransduction.* . J Biol Chem. 1995;270(27):16147–52. PubMed PMID: 7608179.
153. Otto-Bruc A.E. et al. *Phosphorylation of photolyzed rhodopsin is calcium-insensitive in retina permeabilized by alpha-toxin.* . Proc Natl Acad Sci U S A. 1998;95(25):15014–9. PubMed PMID: 9844007.
154. Makino C.L. et al. *Recoverin regulates light-dependent phosphodiesterase activity in retinal rods.* . J Gen Physiol. 2004;123(6):729–41. PubMed PMID: 15173221.
155. Xu J. et al. *Prolonged photoresponses in transgenic mouse rods lacking arrestin.* . Nature. 1997;389(6650):505–9. PubMed PMID: 9333241.
156. Burns M.E. et al. *Deactivation of phosphorylated and nonphosphorylated rhodopsin by arrestin splice variants.* . J Neurosci. 2006;26(3):1036–44. PubMed PMID: 16421323.
157. Smith W.C. et al. *A splice variant of arrestin. Molecular cloning and localization in bovine retina.* . J Biol Chem. 1994;269(22):15407–10. PubMed PMID: 7515057.
158. Palczewski K. et al. *Characterization of a truncated form of arrestin isolated from bovine rod outer segments.* . Protein Sci. 1994;3(2):314–24. PubMed PMID: 8003967.
159. Pulvermuller A. et al. *Functional differences in the interaction of arrestin and its splice variant, p44, with rhodopsin.* . Biochemistry. 1997;36(30):9253–60. PubMed PMID: 9230059.
160. Langlois G. et al. *Responses of the phototransduction cascade to dim light.* . Proc Natl Acad Sci U S A. 1996;93(10):4677–82. PubMed PMID: 8643463.
161. Broekhuysen R.M. et al. *Light induced shift and binding of S-antigen in retinal rods.* . Curr Eye Res. 1985;4(5):613–8. PubMed PMID: 2410196.
162. Mangini N.J., Pepperberg D.R. *Immunolocalization of 48K in rod photoreceptors. Light and ATP increase OS labeling.* . Invest Ophthalmol Vis Sci. 1988;29(8):1221–34. PubMed PMID: 3138199.
163. Philp N.J., Chang W., Long K. *Light-stimulated protein movement in rod photoreceptor cells of the rat retina.* . FEBS Lett. 1987;225(1-2):127–32. PubMed PMID: 2826235.
164. Whelan J.P., McGinnis J.F. *Light-dependent subcellular movement of photoreceptor proteins.* . J Neurosci Res. 1988;20(2):263–70. PubMed PMID: 3172281.

165. Craft C.M., Whitmore D.H. *The arrestin superfamily: cone arrestins are a fourth family.* . FEBS Lett. 1995;362(2):247–55. PubMed PMID: 7720881.
166. Murakami A.et al. *X-arrestin: a new retinal arrestin mapping to the X chromosome.* . FEBS Lett. 1993;334(2):203–9. PubMed PMID: 8224247.
167. Zhu, X., et al., *Rod arrestin expression and function in cone photoreceptors.* Invest. Ophthalmol. Vis. Sci., 2005. 46: p. E-Abstract 1179.
168. Nikonov S.S.et al. *Mouse cones require an arrestin for normal inactivation of phototransduction.* . Neuron. 2008;59(3):462–74. PubMed PMID: 18701071.
169. He W., Cowan C.W., Wensel T.G. *RGS9, a GTPase accelerator for phototransduction.* . Neuron. 1998;20(1):95–102. PubMed PMID: 9459445.
170. Makino E.R.et al. *The GTPase activating factor for transducin in rod photoreceptors is the complex between RGS9 and type 5 G protein beta subunit.* . Proc Natl Acad Sci U S A. 1999;96(5):1947–52. PubMed PMID: 10051575.
171. Hu G., Wensel T.G. *R9AP, a membrane anchor for the photoreceptor GTPase accelerating protein, RGS9-1.* . Proc Natl Acad Sci U S A. 2002;99(15):9755–60. PubMed PMID: 12119397.
172. Chen C.K.et al. *Slowed recovery of rod photoresponse in mice lacking the GTPase accelerating protein RGS9-1.* . Nature. 2000;403(6769):557–60. PubMed PMID: 10676965.
173. Chen C.K.et al. *Instability of GGL domain-containing RGS proteins in mice lacking the G protein beta-subunit Gbeta5.* . Proc Natl Acad Sci U S A. 2003;100(11):6604–9. PubMed PMID: 12738888.
174. Keresztes G.et al. *Absence of the RGS9.Gbeta5 GTPase-activating complex in photoreceptors of the R9AP knockout mouse.* . J Biol Chem. 2004;279(3):1581–4. PubMed PMID: 14625292.
175. Krispel C.M.et al. *Novel form of adaptation in mouse retinal rods speeds recovery of phototransduction.* . J Gen Physiol. 2003;122(6):703–12. PubMed PMID: 14610022.
176. Angleson J.K., Wensel T.G. *Enhancement of rod outer segment GTPase accelerating protein activity by the inhibitory subunit of cGMP phosphodiesterase.* . J Biol Chem. 1994;269(23):16290–6. PubMed PMID: 8206935.
177. Skiba N.P., Hopp J.A., Arshavsky V.Y. *The effector enzyme regulates the duration of G protein signaling in vertebrate photoreceptors by increasing the affinity between transducin and RGS protein.* . J Biol Chem. 2000;275(42):32716–20. PubMed PMID: 10973941.
178. Cowan C.W.et al. *High expression levels in cones of RGS9, the predominant GTPase accelerating protein of rods.* . Proc Natl Acad Sci U S A. 1998;95(9):5351–6. PubMed PMID: 9560279.
179. Zhang X., Wensel T.G., Kraft T.W. *GTPase regulators and photoresponses in cones of the eastern chipmunk.* . J Neurosci. 2003;23(4):1287–97. PubMed PMID: 12598617.
180. Krispel C.M.et al. *Prolonged photoresponses and defective adaptation in rods of Gbeta5<sup>-/-</sup> mice.* . J Neurosci. 2003;23(18):6965–71. PubMed PMID: 12904457.
181. Nikonov S., Engheta N., Pugh E.N. Jr. *Kinetics of recovery of the dark-adapted salamander rod photoresponse.* . J Gen Physiol. 1998;111(1):7–37. PubMed PMID: 9417132.
182. Pepperberg D.R.et al. *Light-dependent delay in the falling phase of the retinal rod photoresponse.* . Vis Neurosci. 1992;8(1):9–18. PubMed PMID: 1739680.
183. Sago M.S., Lagnado L. *G-protein deactivation is rate-limiting for shut-off of the phototransduction cascade.* . Nature. 1997;389(6649):392–5. PubMed PMID: 9311782.
184. Cooper N.et al. *The bovine rod outer segment guanylate cyclase, ROS-GC, is present in both outer segment and synaptic layers of the retina.* . J Mol Neurosci. 1995;6(3):211–22. PubMed PMID: 8672403.
185. Liu X.et al. *Ultrastructural localization of retinal guanylate cyclase in human and monkey retinas.* . Exp Eye Res. 1994;59(6):761–8. PubMed PMID: 7698269.
186. Lowe D.G.et al. *Cloning and expression of a second photoreceptor-specific membrane retina guanylyl cyclase (RetGC), RetGC-2.* . Proc Natl Acad Sci U S A. 1995;92(12):5535–9. PubMed PMID: 7777544.
187. Baehr W.et al. *The function of guanylate cyclase 1 and guanylate cyclase 2 in rod and cone photoreceptors.* . J Biol Chem. 2007;282(12):8837–47. PubMed PMID: 17255100.

188. Yang R.B. et al. *Disruption of a retinal guanylyl cyclase gene leads to cone-specific dystrophy and paradoxical rod behavior.* . J Neurosci. 1999;19(14):5889–97. PubMed PMID: 10407028.
189. Burns M.E., Baylor D.A. *Activation, deactivation, and adaptation in vertebrate photoreceptor cells.* . Annu Rev Neurosci. 2001;24:779–805. PubMed PMID: 11520918.
190. Fain G.L. et al. *Adaptation in vertebrate photoreceptors.* . Physiol Rev. 2001;81(1):117–151. PubMed PMID: 11152756.
191. Cuenca N. et al. *The localization of guanylyl cyclase-activating proteins in the mammalian retina.* . Invest Ophthalmol Vis Sci. 1998;39(7):1243–50. PubMed PMID: 9620085.
192. Howes K. et al. *Gene array and expression of mouse retina guanylate cyclase activating proteins 1 and 2.* . Invest Ophthalmol Vis Sci. 1998;39(6):867–75. PubMed PMID: 9579466.
193. Mendez A. et al. *Role of guanylate cyclase-activating proteins (GCAPs) in setting the flash sensitivity of rod photoreceptors.* . Proc Natl Acad Sci U S A. 2001;98(17):9948–53. PubMed PMID: 11493703.
194. Haeseleer F. et al. *Molecular characterization of a third member of the guanylyl cyclase-activating protein subfamily.* . J Biol Chem. 1999;274(10):6526–35. PubMed PMID: 10037746.
195. Krylov D.M. et al. *Mapping sites in guanylyl cyclase activating protein-1 required for regulation of photoreceptor membrane guanylyl cyclases.* . J Biol Chem. 1999;274(16):10833–9. PubMed PMID: 10196159.
196. Dizhoor A.M. et al. *The human photoreceptor membrane guanylyl cyclase, RetGC, is present in outer segments and is regulated by calcium and a soluble activator.* . Neuron. 1994;12(6):1345–52. PubMed PMID: 7912093.
197. Laura R.P., Hurley J.B. *The kinase homology domain of retinal guanylyl cyclases 1 and 2 specifies the affinity and cooperativity of interaction with guanylyl cyclase activating protein-2.* . Biochemistry. 1998;37(32):11264–71. PubMed PMID: 9698373.
198. Howes K.A. et al. *GCAP1 rescues rod photoreceptor response in GCAP1/GCAP2 knockout mice.* . Embo J. 2002;21(7):1545–54. PubMed PMID: 11927539.
199. Pennesi M.E. et al. *Guanylate cyclase-activating protein (GCAP) 1 rescues cone recovery kinetics in GCAP1/GCAP2 knockout mice.* . Proc Natl Acad Sci U S A. 2003;100(11):6783–8. PubMed PMID: 12732716.
200. Makino C.L. et al. *A role for GCAP2 in regulating the photoresponse. Guanylyl cyclase activation and rod electrophysiology in GUCA1B knock-out mice.* . J Biol Chem. 2008;283(43):29135–43. PubMed PMID: 18723510.
201. Kawamura, S., et al., *Mechanism of rapid visual pigment phosphorylation in carp cones.* Invest. Ophthalmol. Vis. Sci., 2004. 45: p. E-Abstract 2207.
202. Shimauchi-Matsukawa Y. et al. *Isolation and characterization of visual pigment kinase-related genes in carp retina: polyphyly in GRK1 subtypes, GRK1A and 1B.* . Mol Vis. 2005;11:1220–8. PubMed PMID: 16402022.
203. Nikonov S.S. et al. *Physiological features of the S- and M-cone photoreceptors of wild-type mice from single-cell recordings.* . J Gen Physiol. 2006;127(4):359–74. PubMed PMID: 16567464.
204. Yau K.W., McNaughton P.A., Hodgkin A.L. *Effect of ions on the light-sensitive current in retinal rods.* . Nature. 1981;292(5823):502–5. PubMed PMID: 6265800.
205. Mears A.J. et al. *Nrl is required for rod photoreceptor development.* . Nat Genet. 2001;29(4):447–52. PubMed PMID: 11694879.
206. Daniele L.L. et al. *Cone-like morphological, molecular, and electrophysiological features of the photoreceptors of the Nrl knockout mouse.* . Invest Ophthalmol Vis Sci. 2005;46(6):2156–67. PubMed PMID: 15914637.
207. Fei Y., Hughes T.E. *Transgenic expression of the jellyfish green fluorescent protein in the cone photoreceptors of the mouse.* . Vis Neurosci. 2001;18(4):615–23. PubMed PMID: 11829307.
208. Rader A.J. et al. *Identification of core amino acids stabilizing rhodopsin.* . Proc Natl Acad Sci U S A. 2004;101(19):7246–51. PubMed PMID: 15123809.
209. Stenkamp D.L., Cameron D.A. *Cellular pattern formation in the retina: retinal regeneration as a model system.* . Mol Vis. 2002;8:280–93. PubMed PMID: 12181523.
210. Lobanova E.S. et al. *Transducin gamma-subunit sets expression levels of alpha- and beta-subunits and is crucial for rod viability.* . J Neurosci. 2008;28(13):3510–20. PubMed PMID: 18367617.

211. Krispel C.M.et al. *Phosducin regulates the expression of transducin betagamma subunits in rod photoreceptors and does not contribute to phototransduction adaptation.* . J Gen Physiol. 2007;130(3):303–12. PubMed PMID: 17724163.
212. Tsang S.H.et al. *GAP-independent termination of photoreceptor light response by excess gamma subunit of the cGMP-phosphodiesterase.* . J Neurosci. 2006;26(17):4472–80. PubMed PMID: 16641226.
213. Zhang Y.et al. *Knockout of GARPs and the beta-subunit of the rod cGMP-gated channel disrupts disk morphogenesis and rod outer segment structural integrity.* . J Cell Sci. 2009;122(Pt 8):1192–200. PubMed PMID: 19339551.
214. Sampath A.P.et al. *Recoverin improves rod-mediated vision by enhancing signal transmission in the mouse retina.* . Neuron. 2005;46(3):413–20. PubMed PMID: 15882641.
215. Lyubarsky A.L.et al. *RGS9-1 is required for normal inactivation of mouse cone phototransduction.* . Mol Vis. 2001;7:71–8. PubMed PMID: 11262419.
216. Gurevich E.V., Gurevich V.V. *Arrestins: ubiquitous regulators of cellular signaling pathways.* . Genome Biol. 2006;7(9):236. PubMed PMID: 17020596.
217. Baylor D.A., Nunn B.J., Schnapf J.L. *The photocurrent, noise and spectral sensitivity of rods of the monkey Macaca fascicularis.* . J Physiol. 1984;357:575–607. PubMed PMID: 6512705.
218. Baylor D.A., Nunn B.J. *Electrical properties of the light-sensitive conductance of rods of the salamander Ambystoma tigrinum.* . J Physiol. 1986;371:115–45. PubMed PMID: 2422346.
219. Brann M.R., Cohen L.V. *Diurnal expression of transducin mRNA and translocation of transducin in rods of rat retina.* . Science. 1987;235(4788):585–7. PubMed PMID: 3101175.

## License

All copyright for chapters belongs to the individual authors who created them. However, for non-commercial, academic purposes, images and content from the chapters portion of Webvision may be used with a non-exclusive rights under a Attribution, [Noncommercial 4.0 International \(CC BY-NC\) Creative Commons license](http://creativecommons.org/licenses/by-nc/4.0/). Cite Webvision, <http://webvision.med.utah.edu/> as the source. Commercial applications need to obtain license permission from the administrator of Webvision and are generally declined unless the copyright owner can/wants to donate or license material. Use online should be accompanied by a link back to the original source of the material. All imagery or content associated with blog posts belong to the authors of said posts, except where otherwise noted.